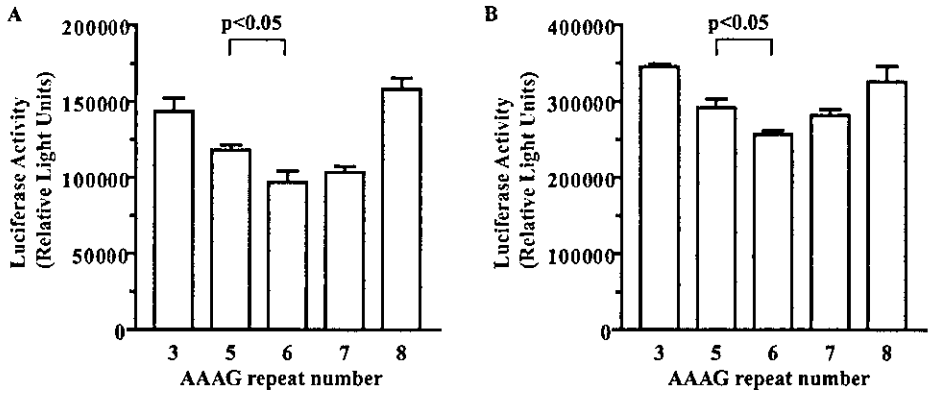

FIG. 5. Effect of the AAAG repeat polymorphism on PTHR P3 promoter activity *in vitro*. The activity of PTHR P3 promoter-luciferase constructs representing all identified polymorphic variants was analyzed in transiently transfected human osteoblastic cell lines as described in *Subjects and Methods*. Transfections were carried out in quadruplicate; each experiment was repeated three times, and independently prepared plasmid DNAs were used for each promoter construct. The mean values of each experiment were combined to determine the mean ± SEM luciferase activity. Luciferase activities are presented in transiently transfected SaOS-2 cells (A) and HOS cells (B) as relative light units (mean ± SEM).

relative expression level of the PTHR1 alleles in chondrocytes and bone cells *in vivo*, then the predicted alterations in PTHR1 levels could be associated with parameters such as adult height and bone formation and resorption in young adults.

Longitudinal growth is under strong genetic control, as evidenced by the effect of parental height on child height and final height attained, which is manifested by developmental canalization in normal height in children (13, 14). The PTHR1, which mediates the effects of PTHrP in the transitional zone of the growth plate, is critical in ensuring the appropriate temporal and spatial control of endochondral bone formation (2, 15, 16). Hence, the PTHR1 gene is a strong candidate to be one of the important factors influencing bone growth and final height. The importance of the PTHR1 in bone growth is well illustrated in two rare genetic disorders, Jansen's metaphyseal chondrodysplasia (17, 18) and Blomstrand lethal chondrodysplasia (BLC) (19, 20). Jansen's metaphyseal chondrodysplasia is characterized by short-limbed dwarfism secondary to severe growth plate abnormalities and increased bone resorption and is due to heterozygous gain of function mutations in the PTHR1 gene giving rise to constitutively active receptors. BLC is characterized by advanced endochondral bone maturation, short-limbed dwarfism, and fetal death and is due to inactivating mutations in the PTHR1 gene. The majority of BLC cases were born to phenotypically normal, consanguineous parents, suggesting an autosomal recessive mode of inheritance. Thus, both loss and gain of function mutations in the PTHR1 give rise to extreme short-limbed dwarfism, which may indicate that fine regulation of PTHR1 expression in the growth plate is critical for optimum height growth. Indeed, in the present study it was found that the PTHR1 genotype was associated with adult stature, with the 6/6 genotype group having a significantly greater mean adult height compared with other groups. In functional studies we demonstrated that this genotype is associated with lower promoter activity, suggesting that a small, but significant, difference in PTHR1 promoter activity could contribute to the difference in adult height.

There was no difference in serum alkaline phosphatase levels among groups, indicating that osteoblast activities with respect to bone formation were not different. However, differences were found with respect to bone resorption markers, and the 6/6 genotype group had lower urinary levels of the collagen breakdown products, deoxypyridinoline and pyridinoline (21). This is likely to represent the role that osteoblastic PTHR1 signaling plays in modulating osteoclastogenesis and/or osteoclast activity via osteoclast differentiation factor and its receptor (22). Cyclical PTH administration in postmenopausal women leads to increased trabecular BMD (23). In addition, suggestive linkage of the PTHR1 locus to BMD was found in subjects (mean age, 50 yr) from families with osteoporosis (24). However, in the present study no differences were observed in BMD at lumbar spine and femoral neck sites among genotype groups. The balance between bone resorption and formation is important in maintaining peak BMD once achieved, but the contribution that PTHR1 makes to the overall process may only become obvious later in life. Therefore, this would not be apparent in the population studied here shortly after achieving peak bone mass.

Serum intact PTH levels were not different among genotypes, suggesting that there was no alteration in parathyroid gland function. However, lower circulating midregion PTH levels were found in the 5/5 genotype group relative to others. This could point to a link between PTHR1 activity in tissues that metabolize PTH (kidney and liver) and the rate at which PTH is cleared from the circulation (25).

In summary, we have identified a polymorphism in a tetranucleotide AAAG repeat region of the human PTHR1 gene promoter that functions as a repressor sequence. Gene transfer experiments showed that promoter recombinant containing the AAAG6 variant displayed the lowest promoter activity. The 6/6 genotype group of a cohort of young adult Japanese women was of significantly greater mean adult height compared with the 5/5 group and had significantly lower levels of urinary markers of bone resorption. These results point to the PTHR1 gene as one of the important genetic factors influencing bone growth and final height.

Acknowledgments

Received February 13, 2001. Accepted January 10, 2002.

Address all correspondence and requests for reprints to: Toshiyuki Yasuda, M.D., Department of Pediatrics, National Chiba Hospital, Tsubakimori, Chuo-ku, Chiba 260-8606, Japan. E-mail: toshi@chiba.hosp.go.jp.

This work was supported by grants from the Japanese Ministry of Education, Culture, Sports, Science, and Technology (12670728); the Japanese Ministry of Health, Labor, and Welfare; the 5th and 6th Novo

Nordisk Awards; and the Novo Nordisk fund for Pediatric Study Group of Molecular Endocrinology.

References

1. **Bringhurst FR, Demay MB, Kronernberg HM** 1998 Hormones and disorders of mineral metabolism. In: Willson JD, Foster DW, Kronenberg HM, Larsen PR, eds. Williams textbook of endocrinology, 9th Ed. Philadelphia: Saunders; 1155–1210
2. **Strewler GJ** 2000 The physiology of parathyroid hormone-related protein. N Engl J Med 342:177–178
3. **Jüppner H** 2000 Role of parathyroid hormone-related peptide and Indian hedgehog in skeletal development. Pediatr Nephrol 14:606–611
4. **Jüppner H, Abou-Samra A-B, Freeman M, Kong XF, Schipani E, Richards J, Kolakowski Jr LF, Hock J, Potts Jr JT, Kronenberg HM, Segre GV** 1991 A G-protein-linked receptor for parathyroid hormone and parathyroid hormone-related peptide. Science 254:1024–1026
5. **Abou-Samra A-B, Jüppner H, Force T, Freeman MW, Kong XF, Schipani E, Urena P, Richards J, Bonventre JV, Potts Jr JT, Kronenberg HM, Segre GV** 1992 Expression cloning of a parathyroid hormone/parathyroid hormone related peptide receptor from rat osteoblast-like cells: a single receptor stimulates intracellular accumulation of both cyclic AMP, and inositol triphosphate and increases intracellular free calcium. Proc Natl Acad Sci USA 89:2732–2736
6. **McCuaig KA, Clarke JC, White JH** 1994 Molecular cloning of the gene encoding the mouse parathyroid hormone/parathyroid hormone-related peptide receptor. Proc Natl Acad Sci USA 91:5051–5055
7. **McCuaig KA, Lee HS, Clarke JC, Assar H, Horsford J, White JH** 1995 Parathyroid hormone/parathyroid hormone related peptide receptor gene transcripts are expressed from tissue-specific and ubiquitous promoters. Nucleic Acids Res 23:1948–1955
8. **Bettoun JD, Minagawa M, Kwan MY, Lee HS, Yasuda T, Hendy GN, Goltzman D, White JH** 1997 Cloning and characterization of the promoter regions of the human parathyroid hormone (PTH)/PTH-related peptide receptor gene: analysis of deoxyribonucleic acid from normal subjects and patients with pseudohypoparathyroidism type 1b. J Clin Endocrinol Metab 82:1031–1040
9. **Bettoun JD, Minagawa M, Hendy GN, Alpert LC, Goodyer CG, Goltzman D, White JH** 1998 Developmental upregulation of human parathyroid hormone (PTH)/PTH-related peptide receptor gene expression from conserved and human-specific promoters. J Clin Invest 102:958–967
10. **Minagawa M, Watanabe T, Kohno Y, Mochizuki H, Hendy GN, Goltzman D, White JH, Yasuda T** 2001 Analysis of the P3 promoter of the human parathyroid hormone (PTH)/PTH-related peptide receptor gene in pseudohypoparathyroidism type 1b. J Clin Endocrinol Metab 86:1394–1397
11. **Takahashi Y, Minamitani K, Kobayashi Y, Minagawa M, Yasuda T, Niimi H** 1996 Spinal and femoral bone mass accumulation during normal adolescence: comparison with female patients with sexual precocity and with hypogonadism. J Clin Endocrinol Metab 81:1248–1253
12. **Minagawa M, Kwan MY, Bettoun JD, Mansour FW, Dassa J, Hendy GN, Goltzman D, White JH** 2000 Dissection of differentially regulated (G+C)-rich promoters of the human parathyroid hormone (PTH)/PTH-related peptide receptor gene. Endocrinology. 141:2410–2421
13. **Reiter EO, Rosenfeld RG** 1998 Normal and aberrant growth. In: Willson JD, Foster DW, Kronenberg HM, Larsen PR, eds. Williams textbook of endocrinology, 9th Ed. Philadelphia: Saunders; 1427–1508
14. **Preece MA** 1996 The genetic contribution to stature. Horm Res 45(Suppl 2):56–58
15. **Karaplis AC, Luz A, Glowacki J, Bronson RT, Tybulewicz VL, Kronenberg HM, Mulligan RC** 1994 Lethal skeletal dysplasia from targeted disruption of the parathyroid hormone-related peptide gene. Genes Dev 8:277–289
16. **Lanske B, Karaplis AC, Lee K, Luz A, Vortkamp A, Pirro A, Karperien M, Defize LH, Ho C, Mulligan RC, Abou-Samra AB, Juppner H, Segre GV, Kronenberg HM** 1996 PTH/PTHrP receptor in early development and Indian hedgehog-regulated bone growth. Science 273:663–666
17. **Schipani E, Langman CB, Parfitt AM, Jensen GS, Kikuchi S, Kooh SW, Cole WG, Jüppner H** 1996 Constitutively activated receptors for parathyroid hormone and parathyroid hormone-related peptide in Jansen's metaphyseal chondrodysplasia. N Engl J Med 335:708–714
18. **Minagawa M, Arakawa K, Takeuchi S, Minamitani K, Yasuda T, Niimi H** 1997 Jansen-type metaphyseal chondrodysplasia: analysis of PTH/PTH-related protein receptor messenger RNA by the reverse transcriptase-polymerase chain method. Endocr J 44:493–499
19. **Jobert AS, Zhang P, Couvineau A, Bonaventure J, Roume J, Le Merrer M, Silve C** 1998 Absence of functional receptors for parathyroid hormone and parathyroid hormone-related peptide in Blomstrand chondrodysplasia. J Clin Invest 102:34–40
20. **Karperien M, van der Harten HJ, van Schooten R, Farih-Sips H, den Hollander NS, Kneppers SL, Nijweide P, Papapoulos SE, Lowik CW** 1999 A frame-shift mutation in the type I parathyroid hormone (PTH)/PTH-related peptide receptor causing Blomstrand lethal osteochondrodysplasia. J Clin Endocrinol Metab 84:3713–3720
21. **Szulc P, Seeman E, Delmas PD** 2000 Biochemical measurements of bone turnover in children and adolescents. Osteop Int 11:281–294
22. **Suda T, Takahashi N, Udagawa N, Jimi E, Gillespie MT, Martin TJ** 1999 Modulation of osteoclast differentiation and function by the new members of tumor necrosis factors and ligand families. Endocr Rev 20:345–357
23. **Hodsman AB, Fraher LJ, Watson PH, Ostbye T, Stitt LW, Adachi JD, Taves DH, Drost D** 1999 A randomized controlled trial to compare efficacy of cyclical parathyroid hormone versus cyclical parathyroid hormone and sequential calciotnin to improve bone mass in post menopausal women with osteoporosis. J Clin Endocrinol Metab 82:620–628
24. **Duncan EL, Brown MA, Sinsheimer J, Bell J, Carr AJ, Wordsworth BP, Wass JA** 1999 Suggestive linkage of the parathyroid receptor type 1 to osteoporosis. J Bone Miner Res 14:1993–1999
25. **Jüppner H, Brown EM, Kronenberg HM** 1999 Parathyroid hormone. In Favus MJ, ed, Primer on the metabolic bone diseases and disorders of mineral metabolism, 4th Ed. Philadelphia: Lippincott-Williams & Wilkins; 80–89

0888-8809/04/$15.00/0
Printed in U.S.A.

Molecular Endocrinology 18(7):1708–1720
Copyright © 2004 by The Endocrine Society
doi: 10.1210/me.2004-0067

Aberrant Dynamics of Histone Deacetylation at the Thyrotropin-Releasing Hormone Gene in Resistance to Thyroid Hormone

S. ISHII, M. YAMADA, T. SATOH, T. MONDEN, K. HASHIMOTO, N. SHIBUSAWA, K. ONIGATA, A. MORIKAWA, AND M. MORI

Department of Medicine and Molecular Science (S.I., M.Y., T.S., T.M., K.H., N.S., M.M.) and Department of Pediatrics and Developmental Medicine (K.O., A.M.), Gunma University Graduate School of Medicine, Maebashi 371-8511, Japan

Histone acetylation status influences transcriptional activity, and the mechanism of negative gene regulation by thyroid hormone remains unclear, although its impairment by a mutant thyroid hormone receptor (TR) is critical for resistance to thyroid hormone (RTH). We found a novel RTH mutant, F455S, that exhibited impaired repression of the TRH gene and had a strong dominant-negative effect on the gene. F455S strongly interacted with nuclear receptor corepressor (NCoR) and was hard to dissociate from it. To analyze the dynamics of histone acetylation status *in vivo*, we established cell lines stably expressing the TRH promoter and wild-type or F455S TR. Treatment with a histone deacetylase (HDAC) inhibitor completely abolished the repression of the gene by T_3. The histones H3 and H4 at the TRH promoter were acetylated, and addition of T_3 caused recruitment of HDACs 2 and 3 within 15 min, resulting in a transient deacetylation of the histone tails. TR and NCoR were located on the promoter, and T_3 caused NCoR dissociation and steroid receptor coactivator-1 recruitment. In the presence of F455S, the histones were hyperacetylated, and HDAC recruitment and histone deacetylation were significantly impaired. This is the first report demonstrating the direct involvement of aberrant dynamics of chromatin modification in RTH. (*Molecular Endocrinology* 18: 1708–1720, 2004)

RESISTANCE TO THYROID hormone (RTH) is an autosomal dominant disorder caused mainly by mutations in the thyroid hormone receptor (TR) β gene (1, 2). RTH is characterized by elevated serum thyroid hormone levels associated with a failure to suppress pituitary TSH secretion. The high levels of thyroid hormone result in various symptoms according to the degree of refractoriness to hormone in peripheral tissues. TRs are members of the nuclear receptor superfamily and function as ligand-regulated transcription factors that increase (positively regulate) or decrease (negatively regulate) the expression of target genes. The serum thyroid hormone levels in RTH patients depend on the resistance in the hypothalamic-pituitary-thyroid hormone axis, in which all critical genes including TRH, TRH-receptor, and TSH genes are negatively regulated by thyroid hormone. Therefore, impairment of the negative gene regulation by thyroid hormone in the hypothalamic-pituitary-thyroid axis plays a critical role in the pathophysiology of RTH.

On the genes positively regulated by thyroid hormone, TR binds to target promoters as a homodimer or a heterodimer with the retinoid X receptor (RXR) and regulates promoter activity by recruiting specific coregulatory protein complexes (3, 4). In the unliganded state, TR assumes a conformation that stably interacts with corepressor molecules such as nuclear receptor corepressor (NCoR) and silencing mediator of retinoic and thyroid hormone receptors (SMRT). Numerous histone deacetylases (HDACs), including HDAC-1, -2, -3, -4, -5, -7, and -9, have been shown to interact with NCoR and SMRT in one context or another, and then repress basal transcriptional activity. Recent chromatin immunoprecipitation (ChIP) experiments have demonstrated that HDAC3 on NCoR, not on SMRT, is most important for the repression by unliganded TR (5).

Stimulation with T_3 leads to the dissociation of corepressors and recruitment of coactivators including members of the p160/steroid receptor coactivator (SRC) family and TR-associated protein/vitamin D receptor-interacting protein mediators. These proteins are thought to function in part by associating with potent histone acetylytransferases (HATs) such as p300/cAMP response element binding protein-binding protein and ultimately import the HAT activity to promoter-bound TR, resulting in the acetylation of nu-

Abbreviations: ChIP, Chromatin immunoprecipitation; FBS, fetal bovine serum; GST, glutathione-S-transferase; HAT, histone acetylytransferase; HDAC, histone deacetylase; NCoR, nuclear receptor corepressor; PML, promyelocytic leukemia; RAR, retinoic acid receptor; RTH, resistance to thyroid hormone; RXR, retinoid X receptor; SDS, sodium dodecyl sulfate; SMRT, silencing mediator of retinoic and thyroid hormone receptor; SRC, steroid receptor coactivator; TR, thyroid hormone receptor; TRE, thyroid hormone receptor response element; TSA, trichostatin A.

***Molecular Endocrinology* is published monthly by The Endocrine Society (http://www.endo-society.org), the foremost professional society serving the endocrine community.**

cleosome histones. Additionally, some p160/SRC family members have intrinsic HAT activity, further supporting a functional role for these factors in chromatin modification (6, 7). It was reported that the ordered recruitment and release of coactivators are important for transcriptional activation (8).

In contrast to the mechanism of positive regulation, the mechanism of trans-repression of the hypothalamic TRH and pituitary TSH subunit genes remains poorly understood. It remains to be elucidated whether direct binding of TR to DNA is necessary for the negative regulation. A detailed analysis of TR knockout mice demonstrated that at least the β isoform of the TR (TRβ) has a key role in the negative feedback regulation of the hypothalamic-pituitary-thyroid axis (9). Although a number of distinct mechanisms for TRβ-mediated negative regulation by thyroid hormone have been proposed, several investigators reported that coregulators including NCoR, SMRT, and SRC-1 are involved in the negative regulation by thyroid hormone and the dominant-negative effect of the mutant TR observed in RTH patients. It is of interest how such cofactors affect histone acetylation status and chromatin structure in the negative gene regulation by thyroid hormone.

In the present study, we first report a novel RTH mutant, F455S, characterized using conventional molecular methods including transient transfection analysis, glutathione-*S*-transferase (GST) pull-down assay, and EMSA. In addition, to investigate the chromatin structure, we established cell lines stably expressing the TRH gene, a typical gene negatively regulated by thyroid hormone, together with the wild-type or mutant TR, and then performed ChIP analysis. We found that transcriptional repression by thyroid hormone of the TRH gene is associated with rapid local histone deacetylation. The dynamics were significantly impaired in the presence of the F455S mutant *in vivo*.

RESULTS

Clinical Studies

A girl, age 11 yr, came to the hospital because of low weight (body mass index, 14.9). She was misdiagnosed as having hyperthyroidism due to Graves' disease. Her blood pressure was 120/80 mm Hg. Her height was 155.1 cm (+1.68 SD) and body weight, 35.8 kg (−0.21 SD). The thyroid gland was enlarged. Her heart rate was 96–120/min. Thyroid function tests revealed the following values: free T_4, 5.7 ng/dl (0.81–2.13); free T_3 ,13.6 pg/ml (2.6–5.4); and TSH, 5.90 μU/ml (0.5–5.5) (Fig. 1A). There was no family history of thyroid disease. She was admitted to the hospital to examine responses to thyroid hormone. After 7 d of treatment with 160 μg T_3, a TRH test showed that the response of serum TSH was not completely depressed, indicating severe RTH (data not shown).

A)

Thyroid Function Tests:

	TSH (μU/ml)	fT4 (ng/dl)	fT3 (pg/ml)
Patient	5.90	5.7	13.6
Mother	1.66	1.2	2.5
Father	0.69	1.66	3.75
Normal range	(0.5-5.5)	(0.81-2.13)	(2.6-5.4)

B)

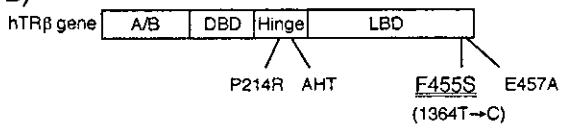

Fig. 1. Thyroid Function in the Family of a Patient with F455S Mutant TRβ (A), and Schematic Representation of the Mutants Used in this Study (B)

Genetic Analyses

Direct sequencing of exon 10 of TRβ in the proband indicated that she was heterozygous for a novel single-nucleotide substitution T to C at nucleotide 1364. The mutation results in the replacement of phenylalanine with serine in codon 455 (F455S) (Fig. 1B). Both parents had a normal TRβ sequence, indicating that the mutation in the patient was sporadic.

F455S TR Mutant Showed Normal T_3 Binding, DNA Binding, and Homo- and Heterodimerization on DNA

The T_3 binding affinity was determined for the F455S mutant and compared with that of the wild-type TR. As shown in Fig. 2A, the T_3 binding affinity of F455S was 86.4% of that of the wild type. Homodimers and heterodimers with RXR of the wild type and F455S were observed in a similar manner in the EMSA study (Fig. 2B).

Transcriptional Activity of the F455S Mutant

To characterize the functional properties of the F455S mutant TR, we compared its ability to modulate the expression of positively and negatively regulated reporter genes in CV1 cells to that of the wild-type TR and TR mutants including E457A, AHT, and P214R. It has been reported that E457A exhibited impaired coactivator binding, and that interaction with corepressors with AHT and P214R was markedly attenuated.

In the first instance, we assayed the ability of mutant receptors to activate transcription of PAL-TK-Luc containing a palindromic TRE (thyroid hormone response element). The wild-type receptor activated PAL-Luc activity in a T_3 dose-dependent manner. Whereas E457A showed almost a complete loss of ability to activate transcription, the stimulation by F455S was

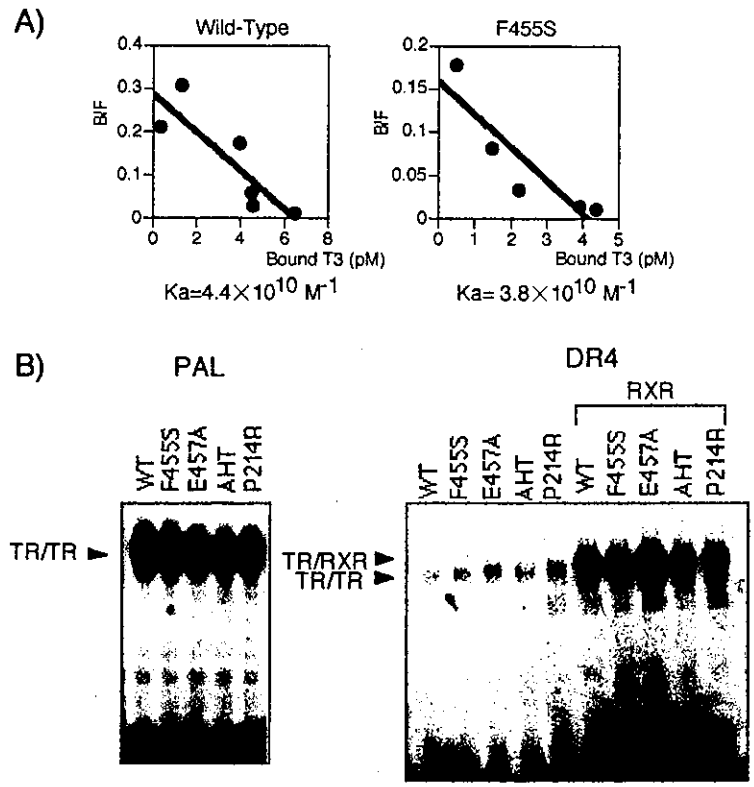

Fig. 2. Scatchard Plot Analysis of T_3 Binding in the Wild-Type (WT) and F455S Mutant TRs (A) and DNA Binding and Dimerization of the Wild-Type and Mutant TRs (B)

EMSA showed normal formation of TRβ homodimers and TR/RXRα heterodimers on palindromic (PAL) (B, *left*) and direct repeat (DR4) (B, *right*) configuration of TRE in all mutant TRs.

significantly impaired at 10 nM and 100 nM T_3 but comparable with that of the wild type in the presence of 1 μM T_3. The ranking in order of activation potency at 1 μM T_3 was F455S>P214R>AHT>E457A (Fig. 3A).

We next performed similar experiments with a reporter gene repressed by the wild-type receptor in a ligand-dependent manner (negatively regulated gene) (Fig. 3B). As previously reported, the promoter region of the TRH gene used in this study contains a typical element negatively regulated by thyroid hormone (10, 11). Expression of the wild-type TR induced a ligand-independent activation that was approximately 2- to 3-fold the basal level (data not shown). Addition of T_3 depressed the activity in a dose-dependent manner with maximal inhibition, 10% of that without T_3, at a concentration of 1 μM. The strongest ligand-independent activation was observed, unexpectedly, when the F455S mutant was expressed, resulting in a 1.5-fold activation compared with the wild type. Furthermore, the inhibition by T_3 was significantly impaired. E457A also exhibited strong ligand-independent activation and impairment of repression by T_3, but the activation was significantly stronger with F455S than with E457A. In contrast, AHT and P214R showed almost no ligand-independent activation and no repression by T_3.

Dominant-Negative Effect of F455S on Positively and Negatively Regulated Promoters

Because a dominant-negative effect is critical to the phenotype and autosomal dominant inheritance of RTH, we investigated the ability to inhibit wild-type receptor action in a dominant-negative manner. In these experiments, equal amounts of wild-type and mutant receptors were coexpressed, and reporter gene activities were assayed at various hormone concentrations. The mutant receptors exhibited a variable spectrum of dominant-negative properties when investigated using PAL-TK-Luc. The greatest dominant-negative effect was observed with E457A, which inhibited the wild-type receptor activation by approximately 80% at 100 nM T_3. The F455S mutant also has a clear dominant effect, showing 40% of inhibition; the AHT mutant did not affect the activation by the wild-type TR, and P214R acted like a wild-type TR (Fig. 4A).

In contrast to the dominant-negative effects on the positively regulated gene, a distinct profile of each mutant was observed for the TRH gene. F455S showed significant dominant-negative activity on repression of the TRH promoter, resulting in a 2.5-fold increase in promoter activity compared with that with

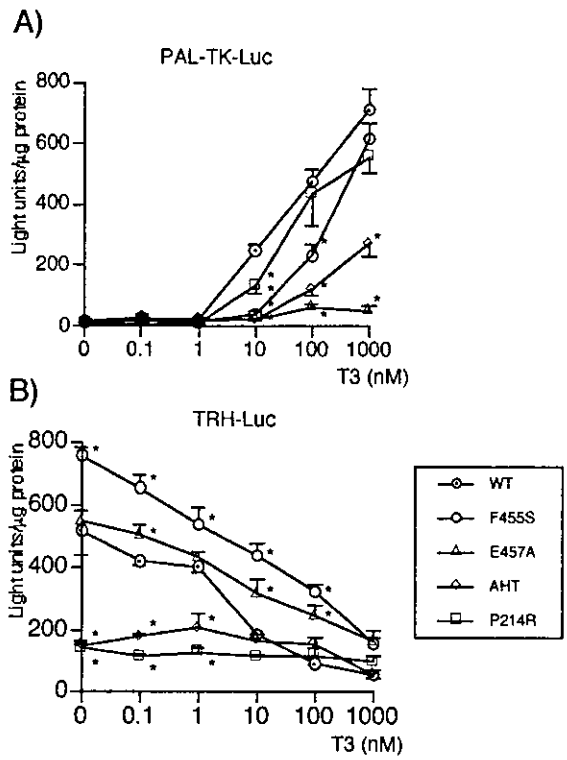

Fig. 3. Transcriptional Properties of the Wild-Type (WT) and Mutant TRs on the Positively Regulated Gene (A) and the TRH Gene (B)

CV-1 cells were transfected with PAL-TK-Luc or TRH-Luc reporter gene and with expression plasmid of wild-type or mutant TR. After incubation with the indicated concentration of T_3 for 48 h, the promoter activity was measured. The data are expressed as the mean ± SE from at least three experiments. *Asterisks* indicate a statistically significant difference ($P < 0.05$) between the wild-type and mutant TRs.

the wild-type TR, even in the presence of 100 nM T_3. At the same T_3 concentration, E457A, AHT, and P214R did not show any effect on the repression by the wild-type TR (Fig. 4B).

NCoR and SRC-1 Binding Properties of Mutant Receptors

We next examined the binding of each mutant to a corepressor, NCoR, and a coactivator, SRC-1. The GST pull-down assay showed that F455S exhibited stronger interaction with NCoR than the wild type, whereas E457A showed a mildly attenuated association. Addition of 1 μM T_3 failed to dissociate NCoR from F455S and led to about 70% dissociation from E457A. EMSA revealed that addition of 10 nM T_3 led to a complete dissociation of NCoR from the wild-type and E457A mutant TRs, but almost no dissociation from the F455S mutant. There was apparent interaction of NCoR with the F455S mutant even at 100 nM T_3. As previously reported, no significant interaction with NCoR was observed in the AHT and P214R mutants with either the GST pull-down assay or EMSA (Fig. 5, A and B).

Both the GST pull-down assay and EMSA showed a significant ligand-dependent association with SRC-1 in the wild-type TR. The interaction of SRC-1 was slightly attenuated in F455S and mildly impaired in P214R. In contrast, the association of SRC-1 with E457A and AHT was markedly impaired (Fig. 6, A and B).

Establishment of GH4C1 Cell Lines Stably Expressing the TRH-Luciferase and the Wild-Type or F455S Mutant TR

Because chromatin modification plays a crucial role in transcriptional regulation, it is necessary to investigate the function of TRs under conditions in which chromatin structure is conserved. We therefore established cell lines stably expressing the TRH promoter gene and either wild-type or F455S mutant TRs, in which we could also examine the TRH promoter activity by the luciferase assay. The single integration of all constructs into genomic DNA was confirmed by Southern blot analysis with the fragment of the luciferase cDNA and TR cDNA as probes (Fig. 7A). Northern blot analysis showed equal expression of the endogenous and exogenous wild-type or F455S TR mRNAs (Fig. 7B), reflecting the pathophysiology of the heterozygote for the F455S mutant. After this Northern blot analysis, we further confirmed by Western blot analysis that equal amounts of TR, including endogenous and exogenous TRs, were expressed in different cell lines (Fig. 7C). Furthermore, the TRH promoter stably expressed in the established cell lines was functionally suppressed by T_3 (Fig. 7D), as observed in the transient transfection analysis shown in Fig. 3B.

Transcriptional Repression Is Associated with Deacetylation of Histones and Recruitment of HDACs at the TRH Promoter

As the SRC-1 complex and NCoR complex possess activity for histone acetylation and deacetylation, we directly analyzed the status of histone at the TRH promoter *in vivo* using ChIP assays with the established cell lines and specific antibodies recognizing acetylated histone H3 and H4 (Fig. 8). Unexpectedly, acetylated histones H3 and H4 were detected in the TRH promoter without stimulation by T_3. Treatment with T_3 caused a significant loss of both acetylated histones H3 and H4 within 15 min. The acetylation level of H3 declined by about 30% within 30 min and recovered to up to 80% of the basal level 120 min after addition of T_3. Histone H4 reached a minimum acetylation level within 15 min (~45% on average) and reacetylation began at 30 min. Histone 4 was completely reacetylated within 120 min. The deacetylation of histones at the TRH promoter suggested that deacetylase complexes should be recruited to this site. Therefore, we performed ChIP analysis with antibodies

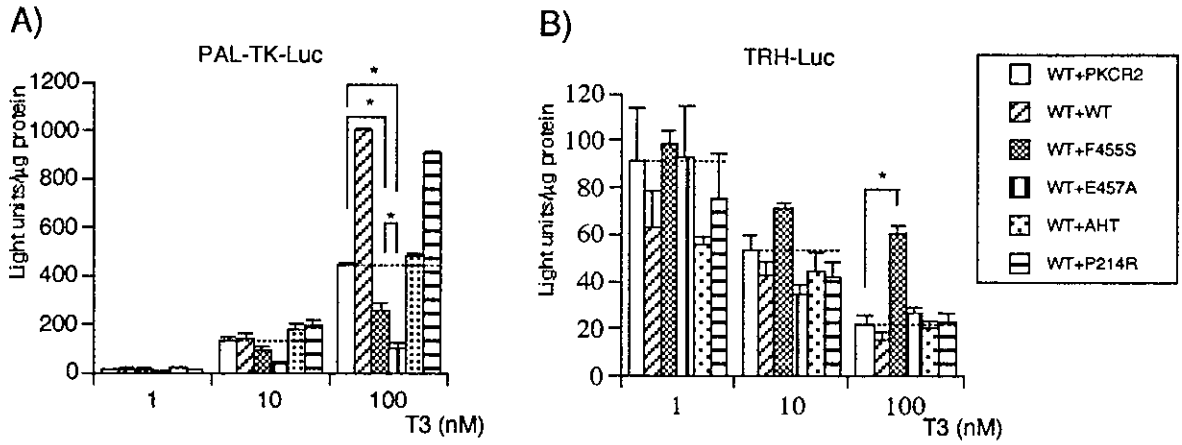

Fig. 4. Dominant-Negative Potencies of the Mutant TRs on the Positively Regulated Genes (A) and the TRH Gene (B)

A, CV-1 cells were transfected with PAL-TK-Luc reporter gene and equal amounts of wild-type (WT) and mutant TR expression vectors. After incubation with the indicated concentration of T_3 for 48 h, the promoter activity was measured. B, The same experiment was performed with TRH-Luc. The data are expressed as the mean ± SE from at least three experiments. *Asterisks* indicate a statistically significant difference ($P < 0.05$) between the wild-type and mutant TRs.

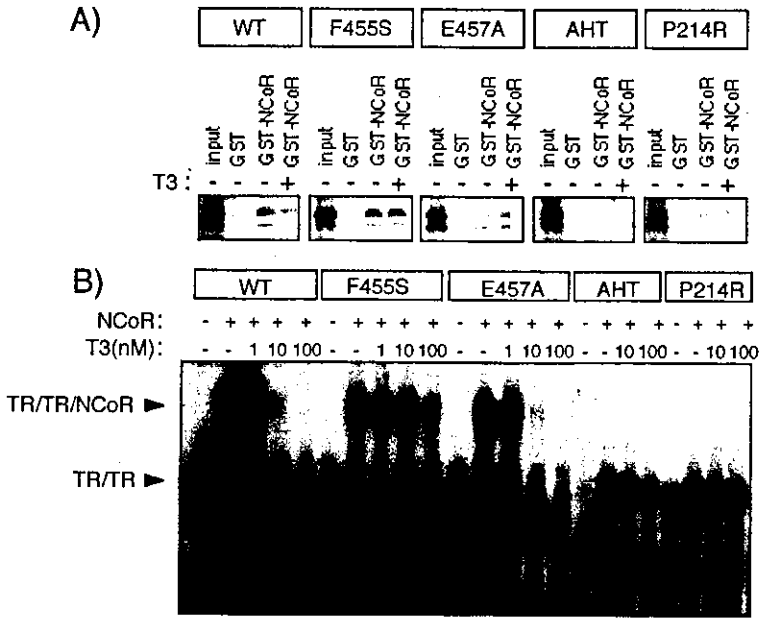

Fig. 5. F455S Exhibited Strong Interaction with and Impaired Dissociation from NCoR

A, GST-pull down assay was performed with ^{35}S-labeled TRs and GST alone (GST) or GST-NCoR fusion proteins in the absence (–) or presence (+) of 100 nM T_3. B, EMSA was performed with ^{32}P-labeled DR4 probe, *in vitro* translated wild-type (WT) or mutant TRs, and the receptor interaction domain of NCoR in the presence of the indicated concentration of T_3. TR homodimers and TR-NCoR complexes on the DNA are indicated by *arrows*. The TR-NCoR complexes dissociated as the concentration of T_3 increased.

against HDACs 1, 2, and 3. The results demonstrated that no HDACs were coprecipitated with the TRH promoter in the absence of T_3. However, addition of T_3 induced a dramatic recruitment of HDACs 3 and 2, particularly HDAC3, on the TRH promoter within 15 min. HDAC3 gradually dissociated and disappeared within 60 min. In contrast, HDAC2 rapidly disappeared from the promoter within 30 min. Interestingly, the dynamics of histone H3 deacetylation and reacetylation correlated well with the recruitment and release of HDAC3, and histone H4 acetylation status seems to be related to the dynamics of HDAC2. These results suggest that nucleosomal changes mediated by transient histone deacetylation with specific histone deacetylases play an important role in mediating the transcriptional repression of the TRH gene by thyroid hormone. Furthermore, the recruit-

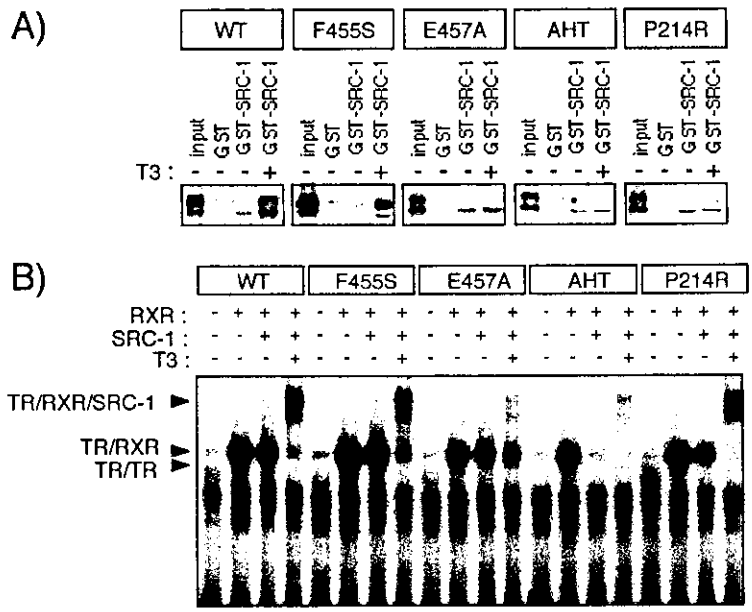

Fig. 6. Interaction with SRC-1 Was Almost Normal in the F455S Mutant

A, GST-pull down assay was performed with ^{35}S-labeled TRs and GST alone (GST) or GST-SRC-1 fusion proteins in the absence (−) or presence (+) of 100 nM T_3. B, EMSA was performed with ^{32}P-labeled DR4 probe, *in vitro* translated wild-type (WT) or mutant TRs, RXR, and the receptor interaction domain of SRC-1 in the absence (−) or presence (+) of 100 nM T_3. TR homodimers, TR/RXR heterodimers, and TR-RXR-SRC-1 complexes on the DNA are indicated by *arrows*.

ment of HDACs was specific, and HDAC1 was not detected in the absence or presence of T_3.

Histone Deacetylase Inhibitor, Trichostatin A (TSA), Abolished TRH Gene Repression by Thyroid Hormone

As this is the first demonstration of the deacetylation of histones and the recruitment of HDACs to the TRH promoter by T_3, we examined the effect of an inhibitor of histone deacetylase, TSA, to assess whether the histone deacetylation was sufficient for the repression of the TRH promoter by thyroid hormone (Fig. 9A). Treatment of the cells with 10 nM TSA did not affect the basal level of the TRH gene promoter activity at all. However, this concentration of TSA completely abolished the repression of the gene induced by thyroid hormone. Furthermore, a higher concentration of TSA (100 nM) induced a nonspecific stimulation of the basal promoter activity probably due to the global inhibition of histone deacetylases. Even at this concentration, the repression of the gene by thyroid hormone was lost. These findings strongly suggested that histone deacetylation is not involved in ligand-independent stimulation by unliganded TR but essential for the TRH gene repression by thyroid hormone.

Unliganded TR and NCoR at the TRH Promoter without T_3 and Recruitment of SRC-1 by T_3

On the positively regulated gene, a recent study utilizing ChIP analysis showed that TR was located on the gene without stimulation by T_3 and that the amount of TR on the gene did not alter even in the presence of T_3 (8). Our assays also demonstrated the occupancy of the TRH promoter by TR in the absence of T_3 and that TR remained on the promoter for more than 120 min.

As on the positively regulated gene, NCoR was also associated with the TRH promoter in the absence of T_3. However, HDACs 1–3 were not detected, suggesting that NCoR was located in the complex on the TRH promoter without the association of HDACs. It is of interest to note that NCoR remained on the promoter even 15 min after addition of T_3, when HDACs were recruited. NCoR then began to dissociate from the TRH promoter at 30 min in parallel with the release of HDAC2 and -3 and disappeared completely in 120 min.

In contrast, SRC-1 was not associated with the promoter in the absence of T_3 but the recruitment of SRC-1 started 30 min after addition of T_3. A significant amount of SRC-1 was detected within 90 min, and then it dissociated again within 120 min (Fig. 9B).

Hyperacetylation and Impaired Deacetylation of Histones at the TRH Gene in Cells Expressing the F455S Mutant TR

To analyze how the chromatin structure is affected on the TRH gene by the presence of the F455S mutant, we also established a cell line stably expressing the mutant. As expected from the strong ligand-independent activation of the TRH promoter by the F455S

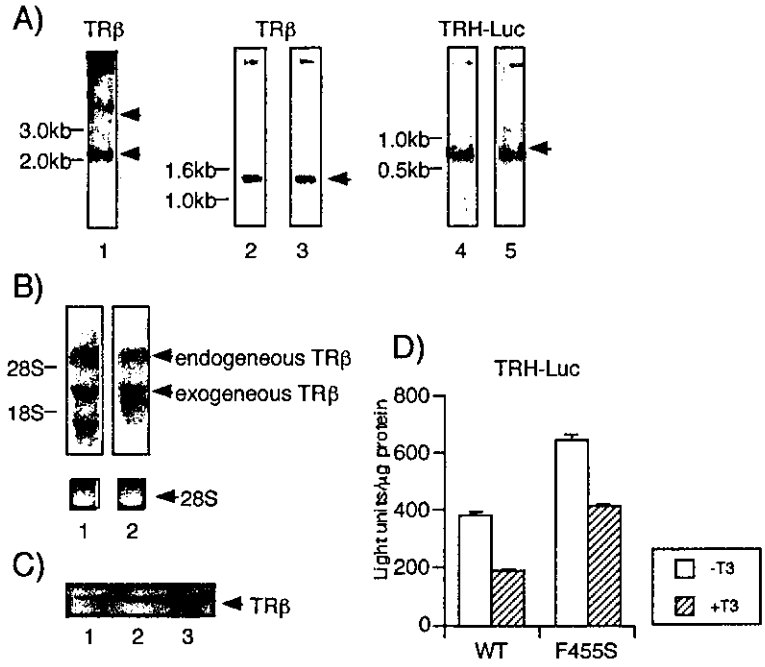

Fig. 7. Establishment of GH4C1 Cell Lines Expressing TRH-Luciferase Reporter Gene and Wild-Type (WT) or F455S Mutant TR

A, GH4C1 cells were stably transfected with TRH-Luc and wild-type or F455S mutant TR along with neomycin-resistant cDNA. After selection with neomycin for 14 d, Southern blot analysis was performed to confirm the single integration of all constructs into the genomic DNA. Representative data are shown here. Approximately 4.0 and 2.2 kb *Hin*dIII-digested fragments of the TR gene were observed in genomic DNA extracted from GH4C1 cells (lane 1). A single 1.4-kb band of the *Eco*R I-digested exogenous TR cDNA was observed in cells transfected with wild-type TR (lane 2) and the F455S mutant (lane 3). The *Bam*HI-digested luciferase cDNA (0.9 kb) were also detected in each cell line (lane 4, wild-type transfected; and lane 5, F455S transfected). B, Northern blot analysis showed equal expression of the endogenous (wild-type) and exogenous (lane 1, wild-type; or lane 2, F455S) mRNA for TRβ in each cell line. C, Western blot analysis revealed that equal amounts of TR proteins were expressed in cells transfected with wild-type TR (lane 2) and the F455S mutant (lane 3). The amount of expression of TR (endogenous and exogenous) was approximately 2 times of that in the nontransfected GH4C1 cells (lane 1). D, The activity of the TRH promoter stably expressed in the established cell lines was functionally suppressed by 100 nM T_3. The data are expressed as the mean ± SE from at least three experiments.

mutant, the degree of histone H3 acetylation at the TRH promoter was significantly higher than that in cells expressing wild-type TR (~140% of the wild-type control) (Fig. 10A). The deacetylation of H3 induced by T_3 was also diminished and delayed: even 60 min after addition of T_3 the acetylation level reached only 80% of the basal level with wild-type TR. In contrast, although the acetylation status of histone H4 in the absence of T_3 was similar to that with the wild-type TR, the deacetylation induced by addition of T_3 was almost completely abolished (Fig. 10B). These results suggested that the hyperacetylation and diminished deacetylation of the histones on the TRH gene are responsible for the impairment of the negative regulation by T_3 in the RTH patient with F455S.

Impairment of HDAC Recruitment with the F455S Mutant

To analyze the mechanism of aberrant acetylation with the mutant TR, we investigated the kinetics of HDACs in the presence of the F455S mutant. ChIP assays revealed that the HDACs examined (HDAC1, -2, and -3) were not detected on the TRH promoter in the absence of T_3 as observed with the wild-type TR. The T_3-induced rapid recruitment of HDAC3 to the TRH promoter was markedly delayed and impaired, the maximum occupancy being achieved 45 min after the addition of T_3 and reaching approximately 75% of that with the wild type. Furthermore, the recruitment of HDAC2 was more severely impaired, resulting in only 40% occupancy of the wild-type control (Fig. 10, C and D). Again, of note is the correlation of the dynamics between HDAC3 and the deacetylation of histone H3, and between HDAC2 and the deacetylation of histone H4.

We finally examined the kinetics of NCoR and SRC-1 on the TRH promoter. Reflecting the results obtained by EMSA and GST pull-down assays, in cells expressing F455S, the occupancy of the TRH promoter by NCoR in the absence of T_3 was markedly increased (~200% of the control), and the maximum dissociation from the gene was also impaired, reaching only the same level as the wild-type TR without T_3.

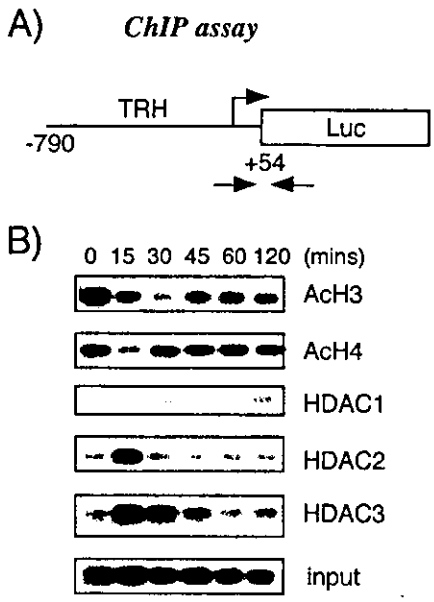

Fig. 8. Histone Deacetylation and Recruitment of HDACs at the TRH Promoter *in Vivo*

A, Schematic representation of the TRH promoter and the luciferase gene integrated into the genomic DNA. *Arrows* indicate the position of primers used for ChIP analysis. B, GH4C1 cells stably expressing the TRH promoter reporter gene and the wild-type (WT) TR were treated with 100 nM T_3 for the indicated period. The time course of the TRH promoter occupancy by acetylated histone 3 (AcH3), histone 4 (AcH4), and HDAC 1, 2, and 3 was analyzed by ChIP assay. Similar results were obtained from at least three independent experiments.

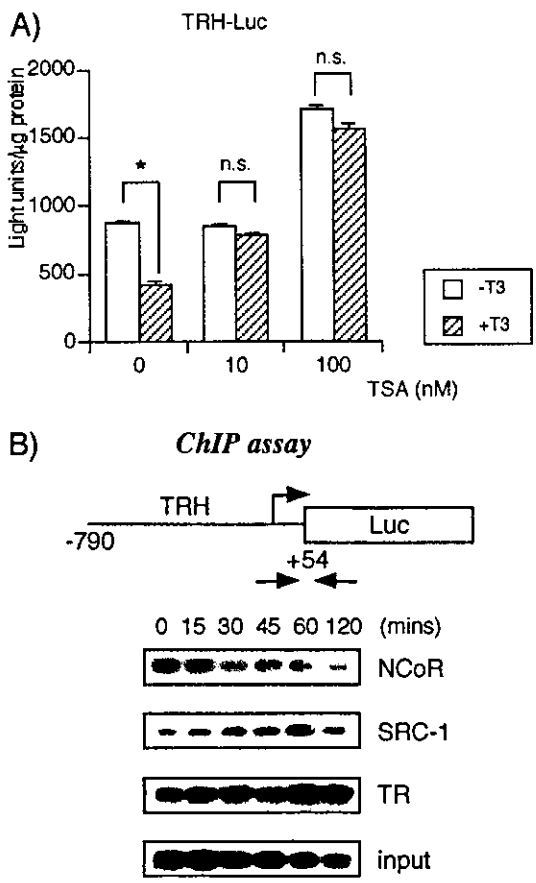

Fig. 9. TSA Abolished TRH Gene Repression by Thyroid Hormone (A) and Ordered Recruitment of TR, NCoR, and SRC-1 Induced by T_3 at the TRH Promoter *in Vivo* (B)

A, GH4C1 cells stably expressing the TRH promoter reporter gene and the wild-type (WT) TR were treated with TSA (10 and 100 nM), and the activity of the TRH promoter was assayed. The data are the mean ± SE from at least three experiments. *Asterisks* indicate a statistically significant difference ($P < 0.01$). B, ChIP assays were performed as in Fig. 8 with specific antibodies against TRβ, NCoR, and SRC-1. Similar results were obtained from at least three independent experiments.

In contrast, the recruitment of SRC-1 was observed in a similar manner as in cells expressing the wild-type TR (Fig. 10, E and F).

DISCUSSION

In this study, we report a novel natural mutation, F455S, in the AF-2 domain of the TRβ gene. It had a stronger affinity for NCoR than the wild-type receptor in the absence of T_3, and the release of NCoR by T_3 was markedly impaired. By ligand binding, the AF-2 domain in helix 12 of the ligand-binding domain has been proposed to come into close contact with helices 3, 5, and 6, creating a small hydrophobic cleft where the transcriptional coactivators bind (12–14). In contrast, the most critical site for NCoR binding overlaps the coactivator binding site but extends underneath helix 12 (15). As shown in Fig. 11, computer analysis revealed that the residue of F455S examined in the present study is localized inside of helix 12 (16, 17). Furthermore, it has been suggested that the presence of helix 12 inhibits NCoR binding to TR, estrogen receptor, and RXR (18–20). On the basis of these observations, it is suggested that helix 12 of F455S cannot be in the position required for suppression of NCoR binding, resulting in the increased interaction with NCoR.

NCoR has been reported to form complexes with several HDACs, and SRC-1 has intrinsic HAT activity and associates with potent HATs. Hence we hypothesized that the characteristic interaction of the F455S mutant with NCoR and SRC-1 may lead to changes in chromatin modification, resulting in the impaired negative gene regulation by thyroid hormone, which play a critical role in the pathophysiology of RTH. Although involvement of HDACs in the negative gene regulation has been reported, precise time course of histone modification and how histone modification was affected in RTH remain unknown. Therefore, we first investigated chromatin modification induced by thy-

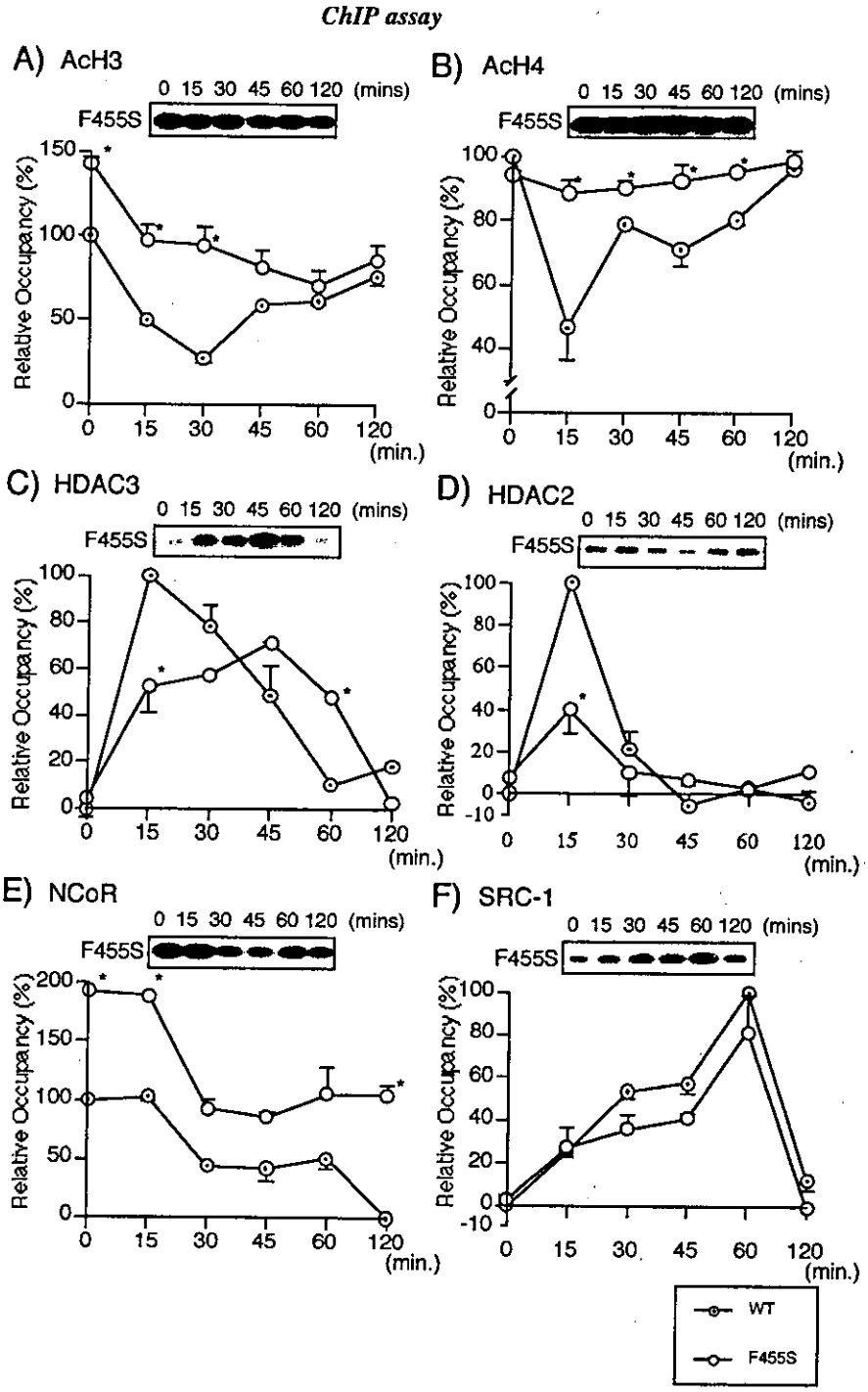

Fig. 10. Hyperacetylation and Aberrant Dynamics of Histone Deacetylation at the TRH Gene in Cells Expressing the F455S Mutant TRs *in Vivo*

ChIP assays were performed as in Fig. 8 with cells expressing F455S mutant TRs and antibodies against AcH3 (A), AcH4 (B), HDAC2 (C), HDAC3 (D), NCoR (E), and SRC-1 (F). Hyperacetylation and impaired deacetylation of histones (A and B) impairment of HDAC recruitment (C and D), and increased recruitment and impaired dissociation of NCoR (E and F) were observed in cells expressing the F455S mutant TRs *in vivo*. The values with AcH3, AcH4, and NCoR antibody were expressed as a percentage of the basal level of the wild type (WT) (100%), and values with HDAC2, HDAC3, and SRC-1 antibody were expressed as a percentage of the peak value of the wild type. The data are represented as the mean ± SE of at least three experiments. *Asterisks* indicate a statistically significant difference ($P < 0.05$) between the wild-type and mutant TR.

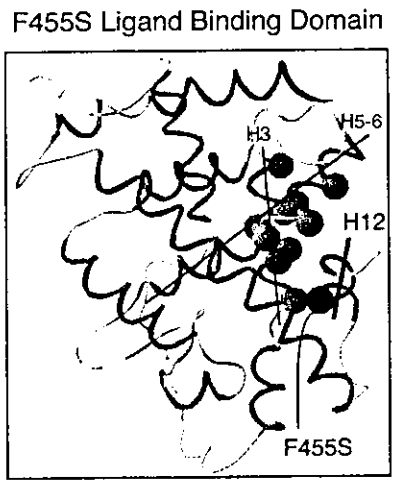

Fig. 11. The F455S Residue Is Localized Inside of Helix 12 of the TR

Estimated ribbon diagram of the ligand-binding domain of the F455S mutant. The F455S residue is presented as a *solid black ball*. Residues present *underneath* helix 12 and reported to be critical for NCoR binding are marked as *solid gray balls*. Computer analysis was done with Swiss-Pdb-Viewer.

roid hormone on the TRH promoter and then demonstrated direct involvement of impaired chromatin modification in the disease. The reason why the TRH gene was selected in this study is that the gene is well characterized as a typical negatively regulated gene by thyroid hormone, and its promoter possesses potent activity compared with the TSAα and -β gene promoters.

Using ChIP analyses, we found that lysine residues of histone H3 and H4 at the TRH promoter were acetylated in the absence of T_3. After addition of T_3, histone tails were rapidly deacetylated within 30 min, and this was correlated with the simultaneous recruitment of HDACs, particularly HDACs 3 and 2. Thus, it is speculated that recruited HDACs deacetylate histone tails on the TRH gene promoter, resulting in repression of the gene. The precise mechanism by which a transient histone deacetylation upon T_3 treatment led to continuous repression over a few days remains to be elucidated. It is possible that cyclic turnover of transcription complex may occur every several hours as recently reported for estrogen receptor (21), or other histone configuration such as methylation, phosphorylation, or chromatin remodeling may be involved in the late stage of the repression. However, our results showing that treatment of a HDAC inhibitor, TSA, completely abolished the repression of the TRH gene indicated that rapid deacetylation of the histone tails of the gene is critical for the transcriptional repression of the TRH gene by thyroid hormone.

One of the remaining questions is how HDACs are recruited to the TRH gene. One possibility is that HDACs are corecruited with NCoR because NCoR has been shown to bind HDAC or Sin3A/HDACs. However, to our surprise, NCoR did not bind HDAC 1–3 on the TRH promoter in the absence of T_3. After addition of T_3, NCoR remained on the gene for approximately 15 min before dissociating, and in this period HDACs were recruited to the gene. Therefore, T_3 may be a trigger for recruitment of HDACs to NCoR on the TRH promoter. Alternatively, HDACs could be recruited by another complex containing specific transcriptional factors, although our attempts to identify the specific recruitment factor are still in progress. Indeed, this is the first demonstration of the presence of NCoR without binding HDACs on the TRH promoter in the absence of T_3 *in vivo*.

After NCoR began to dissociate, HAT SRC-1 was recruited to the TRH promoter. The appearance of SRC-1 correlated well with the reacetylation of histones, suggesting that the reacetylation was induced, at least in part, by the recruitment of SRC-1. In addition, it is of interest that the recruited SRC-1 started to dissociate again after 90 min. Recent analyses on positively regulated genes (dio1 and SERCA gene) revealed the same dissociation, and acetylated H4 was observed even after the dissociation (8). On the basis of these findings and our results, SRC-1 is thought to be necessary for the initiation of histone acetylation but not for the maintenance of acetylated histones on the TRH promoter.

To explain the negative regulation of the gene expression by thyroid hormone, both DNA binding-dependent and -independent mechanisms have been proposed (22–25). Recent analysis demonstrated that the negative thyroid hormone receptor response element (TRE) on the GH promoter bound to TR, and that T_3 causes the release of TR as well as disappearance of acetylated histone from the promoter (26). They also demonstrated the importance of HDAC1 for this repression. Therefore, the mechanism of the negative regulation of the GH gene by thyroid hormone is completely different from that of the TRH promoter gene observed in this study, suggesting that there would be several distinct mechanisms involved in the negative regulation of each gene by thyroid hormone.

Previous studies revealed that NCoR acted as a coactivator on the negative TRE (22, 23, 27). Reflecting the nature of F455S, which strongly interacts with and is hard to dissociate from NCoR, our ChIP analyses demonstrated that the occupancy of the TRH promoter by NCoR was significantly increased in the presence of F455S. These observations suggested that the increased amount of NCoR may affect the histone hyperacetylation at the TRH promoter in the absence of T_3, and that dissociation of NCoR may contribute to the transcriptional repression. Furthermore, these results suggested direct interaction of TR and NCoR in the complex on the TRH promoter *in vivo*. Taken together, these observations indicate that the abnormal histone acetylation status of the TRH promoter in the presence of F455S is responsible for the impairment of the negative regulation of TRH expression by thyroid hormone.

Another example of a disorder related to aberrant interaction with NCoR is acute promyelocytic leukemia (PML). In this case, key molecular events are caused by chromosomal rearrangements of the retinoic acid receptor (RAR), resulting in the fusion gene transcript PML-RARα (28). RARα in PML-RARα shows stronger interaction with NCoR, but the target genes of PML-RARα remain obscure. Therefore, our present study on RTH demonstrated the first direct involvement of the disturbance of the chromatin structure on the targeted gene with the human disorder *in vivo*. We propose a new category of diseases: RTH is a chromatin structure disease as well as a genetic disease.

MATERIALS AND METHODS

Genetic Studies

With informed consent, genomic DNA was extracted from the leukocytes of a patient and her parents. The study protocol was approved by the ethics committees of the Gunma University School of Medicine. The coding exons of the human TRβ gene were amplified using PCR and were sequenced in the sense and antisense direction using an autosequencer (PRISMTM 310, Applied Biosystems, Foster City, CA).

Mammalian Cell Culture and Transfection

CV-1 cells and GH4C1 cells were grown in DMEM supplemented with 10% fetal bovine serum (FBS), as described previously (29). Cells were split into six-well plates at subconfluency 24 h before transfection. The transient transfection was performed using a calcium phosphate precipitation method, as described previously (29). The total amount of transfected plasmid was adjusted by adding an empty expression vector in all experiments. After transfection (16 h), the medium was changed to DMEM supplemented with 10% FBS and treated with AG1-X8 resin (Bio-Rad Laboratories, Inc., Hercules, CA) and activated charcoal (Sigma Chemical Co., St. Louis, MO) to remove thyroid hormones. Cells were further incubated in the absence or presence of T_3 (Sigma).

For stable transfection, cells were grown in 100-mm diameter dishes and cotransfected with 6.7 μg of each linearized plasmid (TRH promoter (−790 +54) luciferase reporter, $pKCR_2$-wild type TR, or $pKCR_2$-F455S TR mutant and pKJ_2-Neo) for 24 h using calcium-phosphate methods. The cells were cultured in complete medium for 48 h before selection using 0.7 mg/ml G-418 sulfate (Life Technologies, Inc., Gaithersburg, MD). In 20 clones tested for reporter activity, integration of the TR or TR F455S gene was examined by extracting genomic DNA and PCR. Southern blot analysis was performed to confirm the single integration of all constructs into the genomic DNA. Luciferase (1–259) and full-length TRβ cDNA fragments were used for probes. Expression levels of each mRNA and protein were examined by Northern blot and Western blot analysis as previously described (29, 30). A cRNA fragment for TRβ (499–835) was used for probes.

Plasmid Constructions

The mutant human $TR\beta_1$ cDNAs (F455S, E457A, P214R, and AHT, which contains three amino acid substitutions in the hinge region) were prepared by PCR mutagenesis and verified by sequencing the DNA. Mutant and wild-type receptor cDNAs were subcloned into the vector $pKCR_2$ for *in vitro* transcription/translation and for transient expression analysis. Firefly luciferase reporter plasmids (pA3Luc) carrying the palindromic (PAL-TK-Luc) or direct repeat-type (DR4) TRE were prepared as previously described (30). TRH-Luc contains 790 bp of the 5′-flanking sequence and 54 bp of exon 1 from the human TRH gene in pA3-Luc (TRH-Luc).

T_3 Binding Experiments

Mutant or wild-type TR was transcribed and translated using a TNT-coupled reticulolysate system (Promega Corp., Madison, WI). T_3-binding affinity was determined using a filter-binding assay as reported previously (31). Fitting with lines in Scatchard plots was done with Cricket Graph (Computer Associates Ltd., Islandia, NY).

EMSA

The EMSA was performed using radiolabeled TRE DR4 or TRE palindrome fragments as described previously (29). The consensus sequences used as TRE DR4 and palindrome were 5′-agcttcaggtcacaggaggtcagagag-3′, and 5′-aagatta-aggtcatgacctgaggaga-3′, respectively. Double-stranded oligonucleotides were labeled with [α^{32}P]dCTP by a fill-in reaction using a Klenow fragment of DNA polymerase I. The binding reaction, gel electrophoreses, and autoradiographies were performed under conditions described previously (29).

GST Pull-Down Assay

[^{35}S] methionine-labeled wild-type and mutant TRβ were synthesized by *in vitro* transcription/translation from $pKCR_2$-TR, F455S, E457A, R214R, and AHT using T_7 RNA polymerase and the TNT-coupled reticulocyte lysate system (Promega Corp.). The synthesis of proteins of expected molecular weights was confirmed by SDS-PAGE). A cDNA fragment encoding the receptor interaction domain of NCoR and SRC-1 was amplified by PCR using $pKCR_2$-NCoRI and $pKCR_2$-SRC-1 as a template and subcloned in frame into pGEX4T1 to yield GST fusion proteins in *Escherichia coli DH5α*. The GST fusion proteins were purified on glutathione-agarose beads (Sigma) and analyzed by SDS-PAGE. Interaction assays and autoradiographies were performed as described previously (30). Bound protein was quantified using a Molecular Imager FX (Bio-Rad).

Luciferase Assay

To determine the luciferase (Luc) activity, cell monolayers were rinsed twice with PBS, and then lysed with 300 μl of 25 mM glycylglycine (pH 7.8) containing 15 mM $MgSO_4$, 4 mM EGTA, 1 mM dithiothreitol, and 1% (vol/vol) Triton X-100. Cells were scraped from the dishes and centrifuged at 12,000 x *g* for 5 min at 4 C. Assays for Luc activity were performed using 150 μl aliquots of cell lysate and 210 μl of 25 mM glycylglycine (pH 7.8) containing 15 mM $MgSO_4$, 4 mM EGTA, 3.3 mM KPO_4, 1 mM dithiothreitol, and 0.45 mM ATP. The reaction was initiated by addition of 200 μl of 0.2 mM D-luciferin, and light emission was measured for 10 sec using a luminometer. Luc activity was expressed as arbitrary light units per μg of cellular protein. All the transfection experiments were repeated at least twice with triplicate determinants.

Antibodies

Antibodies against TRβ (no. 06-539), acetylated Histone H3 (no. 06-599) and H4 (no. 06-866) were obtained from Upstate Biotechnology, Inc. (Lake Placid, NY). Antibodies against HDAC1 (H-51), HDAC2 (H-54), HDAC3 (H-99), NCoR (C-20),

and SRC-1(N-19) were obtained form Santa Cruz Biotechnology, Inc. (Santa Cruz, CA).

ChIP Assay

ChIP analyses were performed according to the manufacturer's instructions (Upstate Biotechnology) with some modifications. Cells (2×10^7) were grown in DMEM supplemented with 10% FBS treated with AG1-X8 resin and activated charcoal for 24 h. After addition of T_3, cells were washed with PBS and treated with the cross-linking reagent formaldehyde (final concentration, 1%) for 10 min at 37 C. They were then rinsed twice with cold PBS containing 0.5 mM phenylmethylsulfonyfluoride and 1 μg/ml of aprotinin. Cells were collected by centrifugation for 4 min at 4 C and resuspended in 150 μl of sodium dodecyl sulfate (SDS) lysis buffer (1% SDS/10 mM EDTA/50 mM Tris-HCl, pH 8.1) with proteinase inhibitors and incubated for 10 min on ice. Samples were sonicated on ice five times for 8 sec each (*i.e.* until the average length of the sheared genomic DNA was 0.2–1.0 kbp) and centrifuged for 10 min. One percent of the supernatant was used as input, and the remaining amount was subjected to the ChIP procedure. Next, 40 μl of salmon sperm DNA/Protein A Agarose-50% slurry were added to reduce the nonspecific background and incubated for 30 min at 4 C with agitation. The solution was then incubated with 1–3 μg of specific antibody or normal IgG and rotated at 4 C overnight. Immunoprecipitated chromatin complexes were isolated by adding 50 μl of salmon sperm DNA/Protein A Agarose-50% slurry and rotating the reactions for 1 h at 4 C. Immunoprecipitates were sequentially washed with low-salt immune complex wash buffer [20 mM Tris-HCl (pH 8.1)/2 mM EDTA/0.1% SDS/1% Triton X-100], followed by high-salt wash buffer [20 mM Tris-HCl (pH 8.1)/2 mM EDTA/0.1% SDS/1% Triton X-100/500 mM NaCl], LiCl Immune complex wash buffer (10 mM Tris-HCl (pH 8.1)/0.25 M LiCl/1% Nonidet P-40/1% deoxycholate/1 mM EDTA) and twice in 1× Tris-EDTA, pH 8.0. To elute the immunoprecipitated chromatin complexes from the resin, 100 μl of elution buffer (1% SDS/0.1 M $NaHCO_3$) were added to the beads, and the tubes were vortexed and incubated at room temperature for 15 min with rotation. The supernatant was then collected, and the elution was repeated with a fresh 100 μl of elution buffer. After combining the eluants in one tube, the protein-DNA cross-linking was reversed by adding 5 M NaCl to a final concentration of 200 mM and heating at 65 C for 4 h. Inputs were diluted to 200 μl and subjected to the same procedure. Each sample was added to 8 μl of 1 M Tris-Cl (pH 6.5), 4 μl of 0.5 M EDTA, and 5 μg of proteinase K (Life Technologies) and subsequently incubated at 45 C for 1 h. Samples were then extracted with phenol/chloroform/isoamylalcohol (25:24:1), and the DNA was precipitated with ethanol and subsequently resuspended in 50 μl H_2O. PCR was performed with 5 μl of immunoprecipitate or input (see above), 0.5 μM of each primer, 1.5 mM $MgCl_2$, 0.2 mM deoxynucleotide triphosphate mixture, 1× thermophilic buffer, and 2.5 U of AmpliTaq DNA polymerase (Applied Biosystems) in a total volume of 50 μl. The primers for the human TRH promoter were: forward, 5′-ctgagcgctgcagactcctgacct-3′; and reverse, 5′-tgttcacctcgatatgtgcatctgt-3′. Initially, PCR was performed with a serial dilution of input DNA to determine the linear range of the amplification for each gene. PCR conditions were 25 cycles of 45 sec at 94 C, 45 sec at 60 C, and 1 min at 72 C. All PCR signals were visualized by Southern blot analysis with the fragment of the TRH-luciferase cDNA (pA3TRH-Luc) as a probe and quantified with the Molecular Imager FX (Bio-Rad). The probe was labeled by the random-priming method with Ready-To-Go DNA Labeling Kit (Pharmacia Biotech, Piscataway, NJ) and [^{32}P]dCTP. The values were corrected using the input values, and those obtained with IgG were used as background values.

Statistical Analysis

Statistical analysis was performed using ANOVA and Student's *t* test or Duncan's multiple range test. The level of significance was set at $P < 0.05$.

Acknowledgments

Received February 16, 2004. Accepted April 14, 2004.

Address all correspondence and requests for reprints to: Masanobu Yamada, M.D., Ph.D., Department of Medicine and Molecular Science, Gunma University Graduate School of Medicine 3-39-15 Showa-machi, Maebashi, Gunma 371-8511, Japan. E-mail: myamada@med.gunma-u.ac.jp.

This work was supported in part by a Health and Labor Sciences Research Grant from the Japanese Ministry of Health, Labor and Welfare.

REFERENCES

1. Refetoff S, Weiss RE, Usala SJ 1993 The syndromes of resistance to thyroid hormone. Endocr Rev 14:348–399
2. Yen PM 2001 Physiological and molecular basis of thyroid hormone action. Physiol Rev 81:1097–1142
3. Zhang J, Lazar MA 2000 The mechanism of action of thyroid hormones. Annu Rev Physiol 62:439–466
4. Yen PM 2003 Molecular basis of resistance to thyroid hormone. Trends Endocrinol Metab 14:327–333
5. Ishizuka T, Lazar MA 2003 The N-CoR/histone deacetylase 3 complex is required for repression by thyroid hormone receptor. Mol Cell Biol 23:5122–5131
6. McKenna NJ, Lanz RB, O'Malley BW 1999 Nuclear receptor coregulators: cellular and molecular biology. Endocr Rev 20:321–344
7. Glass CK, Rosenfeld MG 2000 The coregulator exchange in transcriptional functions of nuclear receptors. Genes Dev 14:121–141
8. Sharma D, Fondell JD 2002 Ordered recruitment of histone acetyltransferases and the TRAP/mediator complex to thyroid hormone-responsive promoters in vivo. Proc Natl Acad Sci USA 99:7934–7939
9. Weiss RE, Forrest D, Pohlenz J, Cua K, Curran T, Refetoff S 1997 Thyrotropin regulation by thyroid hormone in thyroid hormone receptor β-deficient mice. Endocrinology 138:3624–3629
10. Hollenberg AN, Monden T, Flynn TR, Boers ME, Cohen O, Wondisford FE 1995 The human thyrotropin-releasing hormone gene is regulated by thyroid hormone through two distinct classes of negative thyroid hormone response elements. Mol Endocrinol 9:540–550
11. Satoh T, Yamada M, Iwasaki T, Mori M 1996 Negative regulation of the gene for the preprothyrotropin-releasing hormone from the mouse by thyroid hormone requires additional factors in conjunction with thyroid hormone receptors. J Biol Chem 271:27919–27926
12. Bourguet W, Ruff M, Chambon P, Gronemeyer H, Moras D 1995 Crystal structure of the ligand-binding domain of the human nuclear receptor RXR-α. Nature 375:377–382
13. Wagner RL, Apriletti JW, McGrath ME, West BL, Baxter JD, Fletterick RJ 1995 A structural role for hormone in the thyroid hormone receptor. Nature 378:690–697
14. Feng W, Ribeiro RC, Wagner RL, Nguyen H, Apriletti JW, Fletterick RJ, Baxter JD, Kushner PJ, West BL 1998 Hormone-dependent coactivator binding to a hydrophobic cleft on nuclear receptors. Science 280:1747–1749
15. Marimuthu A, Feng W, Tagami T, Nguyen H, Jameson JL, Fletterick RJ, Baxter JD, West BL 2002 TR surfaces and conformations required to bind nuclear receptor corepressor. Mol Endocrinol 16:271–286

16. Guex N, Peitsch MC 1997 SWISS-MODEL and the Swiss-PdbViewer: an environment for comparative protein modelling. Electrophoresis 18:2714–2723
17. Peitsch MC 1996 ProMod and Swiss-Model: Internet-based tools for automated comparative protein modelling. Biochem Soc Trans 24:274–279
18. Webb P, Nguyen P, Kushner PJ 2003 Differential SERM effects on corepressor binding dictate ERα activity in vivo. J Biol Chem 278:6912–6920
19. Zhang J, Hu X, Lazar MA 1999 A novel role for helix 12 of retinoid X receptor in regulating repression. Mol Cell Biol 19:6448–6457
20. Renaud JP, Rochel N, Ruff M, Vivat V, Chambon P, Gronemeyer H, Moras D 1995 Crystal structure of the RAR-γ ligand-binding domain bound to all-trans retinoic acid. Nature 378:681–689
21. Shang Y, Hu X, DiRenzo J, Lazar MA, Brown M 2000 Cofactor dynamics and sufficiency in estrogen receptor-regulated transcription. Cell 103:843–852
22. Tagami T, Madison LD, Nagaya T, Jameson JL 1997 Nuclear receptor corepressors activate rather than suppress basal transcription of genes that are negatively regulated by thyroid hormone. Mol Cell Biol 17: 2642–2648
23. Tagami T, Park Y, Jameson JL 1999 Mechanisms that mediate negative regulation of the thyroid-stimulating hormone α gene by the thyroid hormone receptor. J Biol Chem 274:22345–22353
24. Shibusawa N, Hashimoto K, Nikrodhanond AA, Liberman MC, Applebury ML, Liao XH, Robbins JT, Refetoff S, Cohen RN, Wondisford FE 2003 Thyroid hormone action in the absence of thyroid hormone receptor DNA-binding in vivo. J Clin Invest 112:588–597
25. Shibusawa N, Hollenberg AN, Wondisford FE 2003 Thyroid hormone receptor DNA binding is required for both positive and negative gene regulation. J Biol Chem 278: 732–738
26. Sanchez-Pacheco A, Aranda A 2003 Binding of the thyroid hormone receptor to a negative element in the basal growth hormone promoter is associated with histone acetylation. J Biol Chem 278:39383–39391
27. Berghagen H, Ragnhildstveit E, Krogsrud K, Thuestad G, Apriletti J, Saatcioglu F 2002 Corepressor SMRT functions as a coactivator for thyroid hormone receptor T3Rα from a negative hormone response element. J Biol Chem 277:49517–49522
28. Lin RJ, Sternsdorf T, Tini M, Evans RM 2001 Transcriptional regulation in acute promyelocytic leukemia. Oncogene 20:7204–7215
29. Ozawa A, Yamada M, Satoh T, Monden T, Hashimoto K, Kohga H, Hashiba Y, Sasaki T, Mori M 2002 Transcriptional regulation of the human PRL-releasing peptide (PrRP) receptor gene by a dopamine 2 receptor agonist: cloning and characterization of the human PrRP receptor gene and its promoter region. Mol Endocrinol 16: 785–798
30. Ishizuka T, Satoh T, Monden T, Shibusawa N, Hashida T, Yamada M, Mori M 2001 Human immunodeficiency virus type 1 Tat binding protein-1 is a transcriptional coactivator specific for TR. Mol Endocrinol 15:1329–1343
31. Inoue A, Yamakawa J, Yukioka M, Morisawa S 1983 Filter-binding assay procedure for thyroid hormone receptors. Anal Biochem 134:176–183

Molecular Endocrinology **is published monthly by The Endocrine Society (http://www.endo-society.org), the foremost professional society serving the endocrine community.**

0013-7227/04/$15.00/0
Printed in U.S.A.

Endocrinology 145(6):2865–2875
Copyright © 2004 by The Endocrine Society
doi: 10.1210/en.2003-1258

Histone Deacetylase Inhibitors Restore Radioiodide Uptake and Retention in Poorly Differentiated and Anaplastic Thyroid Cancer Cells by Expression of the Sodium/Iodide Symporter Thyroperoxidase and Thyroglobulin

FUMIHIKO FURUYA, HIROKI SHIMURA, HIDEYO SUZUKI, KATSUMI TAKI, KAZUYASU OHTA, KAZUTAKA HARAGUCHI, TOSHIMASA ONAYA, TOYOSHI ENDO, AND TETSURO KOBAYASHI

Third Department of Internal Medicine, Faculty of Medicine, University of Yamanashi, Yamanashi 409-3898, Japan

Iodide uptake by the thyroid is mediated by the sodium/iodide symporter. Upon iodide uptake, thyroperoxidase catalyzes iodination of tyrosine residues in thyroglobulin, retaining iodide within thyroid follicles. Dedifferentiation-induced loss of these functions in cancers, rendering them unresponsive to radioiodide, occurs with most poorly differentiated and anaplastic tumors. We focused on the histone deacetylase (HDAC) inhibitors (HDACI) as a way to induce differentiation of thyroid cancer cells. We assessed re-expression of thyroid-specific genes mRNA induced by HDACI using quantitative RT-PCR and immunostaining in poorly differentiated papillary and anaplastic thyroid cancer cells. HDACI induced expression of thyroid-specific gene mRNAs and proteins, and accumulation of radioiodide through iodination of generic cellular proteins were detected. HDACI-treated tumors could specifically accumulate ^{125}I as revealed by imaging experiments and radioiodide concentration *in vivo*. In an attempt to determine the mechanism by which these gene expressions occurred, we detected the inhibition of protein synthesis by cycloheximide, which up-regulated the expression of thyroperoxidase and thyroglobulin mRNA in HDACI-treated cells and down-regulated that of sodium/iodide symporter mRNA. Together, our results suggest that HDACI-induced expression of thyroid-specific genes, some of which is mediated by some protein synthesis, may contribute to development of novel strategy against thyroid cancer. (*Endocrinology* 145: 2865–2875, 2004)

THE THYROID GLAND, a relatively common site for development of malignant neoplasms, gives rise to 90% of all endocrine cancers (1). In general, thyroid cancer is a disease with a good prognosis. However, anaplastic thyroid carcinoma constitutes about 5–14% of all thyroid carcinomas and is highly malignant, with a median survival of 2–6 months, rapidly invading adjacent structures, and metastasizing throughout the body, especially to the lung (2, 3). Because no effective therapy is available for patients with these aggressive types of thyroid carcinoma, development of novel therapeutic strategies, including gene therapy, is an urgent priority.

A unique property of thyroid follicular cells is the ability to trap and concentrate iodide, which depends on expression of the sodium/iodide symporter (NIS), thyroglobulin (Tg), and thyroperoxidase (TPO) (4). Several reports indicated that, because of ability for iodide trapping and concentration, radioiodide is an effective therapy in the treatment of differentiated thyroid carcinomas (5–7). NIS protein mediates iodide uptake in normal and well-differentiated neoplastic thyroid cells. TPO iodinates Tg, which leads to iodide retention within thyroid follicles. Concentration of these thyroid-specific functions suggests that restoring lost expression of NIS, TPO, and Tg could provide a basis for radioiodide treatment of thyroid carcinomas. Loss of thyroid-specific functions associated with dedifferentiation in poorly differentiated and anaplastic thyroid cancer cells ordinarily renders them unresponsive to radioiodide therapy. We reported that $Na^{131}I$ administration did not decrease volumes of experimental tumors formed by malignantly transformed rat thyroid cells Tc-rNIS that were stably transfected with rat NIS cDNA but possessed no TPO or Tg expression (8). Concomitant re-expression of NIS, TPO, and Tg therefore would seem necessary for the iodide uptake and retention that could permit effective radioiodide therapy.

Histone acetylation is known to induce changes in nucleosomal conformation that make DNA more accessible to transcription factors (9). Acetylation of histone lysine residues reduces the overall positive charge of the histone, and thus decreases its affinity for the negatively charged DNA molecule (10). Recent reports have shown that histone deacetylase (HDAC) inhibitors (HDACI) can induce expression of silenced genes in cancer cells (11). In bladder carcinoma cells, for example, the HDACI, suberoylanilide hydroxamine acid, induces an increase in $p21^{WAF1}$ mRNA and

Abbreviations: DMSO, Dimethylsulfoxide; GAPDH, glyceraldehyde 3-phosphate dehydrogenase; HBSS, Hanks' balanced salt solution; HDAC, histone deacetylase(s); HDACI, HDAC inhibitor(s); MMI, methimazole; NIS, sodium/iodide symporter; Tg, thyroglobulin; TPO, thyroperoxidase; TSA, trichostatin A; TSH-R, TSH receptor; TTF, thyroid transcription factor.

Endocrinology is published monthly by The Endocrine Society (http://www.endo-society.org), the foremost professional society serving the endocrine community.

protein. Thus, HDACI-induced restoration of tumor suppression- or apoptosis-inducing genes in poorly differentiated cancer, including thyroid cancer, might offer a novel therapeutic strategy.

To develop a way to sensitize anaplastic thyroid carcinoma to radioiodide therapy, we investigated re-expression of thyroid-specific genes, NIS, TPO, and Tg, induced by HDACI. We then examined radioiodide uptake and organification to confirm the function of the re-expressed thyroid-specific genes *in vitro* and *in vivo* models.

Expression of thyroid-specific genes is controlled by the interaction of a complement of thyroid-specific transcription factors with their respective promoters (12–22). At least three transcription factors have been identified: thyroid transcription factor (TTF)-1 (12), TTF-2 (20), and Pax-8 (23). TTF-1, a homeodomain-containing transcription factor expressed in thyroid and lung (12, 24), interacts with all thyroid-specific genes important for thyroid function (12, 13, 16–19). Pax-8, a member of the family of paired box-containing genes, is expressed in the thyroid and kidney (16, 23) and binds to promoter and enhancer sequences in thyroid-specific genes (15, 21, 22, 25). We recently demonstrated that overexpression of TTF-1 could restore Tg promoter activity in Tg-nonproducing poorly differentiated thyroid cancer cell lines, which suggested that TTF-1 is important in the restoration of thyroid-specific gene expression in thyroid cancer cells (24). In an attempt to determine the mechanism by which HDACI induce restoration of thyroid-specific gene expression, we characterized the effect of HDACI on expression of thyroid-specific transcription factors.

Materials and Methods

Reagents

Depsipeptide (FR901228, FK228) was a gift from Fujisawa Pharmaceutical Co. Ltd. (Osaka, Japan). A 1-mg/ml solution of depsipeptide was prepared dimethylsulfoxide (DMSO).

Cell culture

BHP18–21v cells, derived from human papillary thyroid cancer, were provided by Dr. J. M. Hershman (Endocrine Research Laboratory, West Los Angeles Veterans Affairs Medical Center, Los Angeles, CA). BHP18–21v cells expressing Pax-8, but neither TTF-1 nor Tg genes, were isolated from BHP18–21 (26). The BHPcell lines were maintained in RPMI 1640 medium supplemented with 10% fetal calf serum. A human anaplastic thyroid carcinoma cell line, ARO (27), that lacks Pax-8, Tg, and NIS and also shows decreased expression of TTF-1, was donated by Dr. H. Namba (Department of Molecular Medicine, Atomic Bomb Disease Institute, Nagasaki University School of Medicine, Nagasaki, Japan) and incubated with RPMI 1640 containing 10% fetal calf serum.

FRTL-Tc cells (28) were grown in Coon's modified Ham's F-12 medium supplemented with 5% calf serum containing a mixture of five hormones: insulin (10 μg/ml), cortisol (0.4 ng/ml), transferrin (5 μg/ml), glycyl-L-histidyl-L-lysine acetate (10 ng/ml), and somatostatin (10 ng/ml). Rat NIS cDNA (−29 to 1975 bp, with A in ATG designated as +1) (29) was subcloned into the eukaryotic expression vector pcDNA3 (Invitrogen, San Diego, CA) and introduced into FRTL-Tc cells by electroporation. Stably transfected cells were selected using G418 and then cloned by limited dilution. The cloned cell line (Tc-rNIS) (8) that exhibited the highest iodide uptake activity was used for the subsequent experiments.

Determination of mRNA levels using real-time kinetic quantitative RT-PCR in vitro and in vivo

In an *in vitro* and *in vivo* study, total RNA was isolated from cultured cells using RNeasy Mini kit (QIAGEN, Hilden, Germany). After quantification by spectrophotometry, 5 μg total RNA was reverse-transcribed into cDNA with 160 μM deoxynucleotide triphosphate, 50 ng random hexamer primers, and 200 U Superscript II, per the manufacturer's recommendations (Invitrogen Corp., Carlsbad, CA). Oligonucleotide primers and TaqMan probes for NIS (30), Tg (31), TPO, and TSH receptor (TSH-R) (32) genes are shown in Table 1. These primers were designed to be intron spanning. The monitoring of negative control for each target showed an absence of carryover. One of each type of amplicon, corresponding to each target, was migrated on agarose gel electrophoresis and showed a unique band at the expected size. The primers and TaqMan probes of TPO gene were designed using the computer program Primer Express (PerkinElmer Corp., PE Applied Biosystems, Foster City, CA).

To normalize differences in the amount of cDNA added to the reactions, amplification of glyceraldehyde 3-phosphate dehydrogenase (GAPDH) was performed as an endogenous control. Primers and probes for GAPDH were purchased from PerkinElmer Corp., PE Applied Biosystems. Quantitative real-time PCR was achieved in 96 sample tubes using the cDNA equivalent of 100 ng with 1× TaqMan Universal PCR Master Mix, 900 nM of each primer, and 250 nM TaqMan probe. The cycling conditions included an initial phase of 2 min at 50 C, followed by 10 min at 95 C required for optimal uracil-*N*-glycosylase enzyme activity, 45 cycles of 15 sec at 95 C, and 1 min at 60 C. Polymerization reactions were performed in a GeneAmp 5700 Sequence Detection System (PerkinElmer Corp., PE Applied Biosystems).

To validate the quantitative PCR method, standard curves for NIS, TPO, Tg, TSH-R, and GAPDH were constructed from cDNA fragments. The efficiency of each standard curve, as determined by its slope, allowed us to quantify the threshold cycle method according to the manufacturer's instructions. The amount of targeted mRNA was determined by standard curve. For each sample, the targeted mRNA amount was divided by GAPDH to determine a normalized ratio. The crossing points were all less than 30 cycles that are in the linear range of amplification.

TABLE 1. Sequences of primers and TaqMan probes

Genes	Gene bank accession no.			Primer and probe
NIS	U66088	Sense	2089–2109	CCATCCTGGATGACAACTTGG
		Antisense	2166–2187	AAAAACAGACGATCCTCATTG
		Probe		FAM-AGAACTCCCCACTGGAAACAAGAAGCCC-TAMRA
TPO	M17755	Sense	2680–2698	ACCTCGACGGTGATTTGCA
		Antisense	2723–2740	CCGCCTGTCTCCGAGATG
		Probe		FAM-TGGACACGCACTGGCACTAAATCCA-TAMRA
Tg	X05615	Sense	262–280	GTGCCCAACGGCAGTGAAGT
		Antisense	326–348	TCTGCTGTTTCTGTAGCTGACAAA
		Probe		FAM-ACAGACAAGCCACAGGCCGTCCT-TAMRA
TSH-R	M32215	Sense	186–203	CCCAGCTTACCGCCCAGT
		Antisense	238–264	TAGAAAATGCATGACTTGGAATAGTTC
		Probe		FAM-CGCAGACTCTGAAGCTTATTGAGACTCACCTG-TAMRA

Detection of TTF-1 and Pax-8 gene expression using RT-PCR

To determine expression of human TTF-1 and Pax-8 in BHP18–21v and ARO cells, 5 μg total RNA was reverse-transcribed as described above. The cDNAs were amplified using the following intron-flanking primers: human TTF-1 5′ (sense),^{512}AACCTGGGCAACATGAGCG-AGCT^{534}; TTF-1 3′ (antisense),^{771}AGCTCGTACACCTGCGCCTGCGA GAAGA^{734}; human Pax-8 5′ (sense),^{10}GATGCCTCACAACTCCATCA-GATC^{33}; and Pax-8 3′ (antisense)^{603}TCATCCATTTTCCTCTTGTC-GCTG^{586}. The amplification reaction was carried out for 30 cycles, and considered at 94 C for 1 min, 60 C for 1 min, and 72 C for 2 min, followed by a final 10 min elongation at 72 C. All PCR products were analyzed by electrophoresis through 2% agarose gels followed by ethidium bromide staining to ensure amplification of the appropriately sized product.

Immunoperoxidase staining of cells

Immunostaining of thyroid cancer cells treated with HDACI was performed to confirm expression of the NIS, TPO, and Tg proteins in response to HDACI. After treatment of the cells, they were fixed for 15 min in −10 C methanol, air-dried, and then washed three times with PBS. The fixed cells were incubated with an anti-Tg monoclonal (Neo-Markers, Fremont, CA), anti-TPO monoclonal (HyTest Ltd, Eurocity, Turku, Finland), or anti-NIS polyclonal antibody (33) for 30 min and washed with three changes of PBS. Cells then were incubated with biotinylated secondary antibody, washed, and exposed to avidin-biotinylated horseradish peroxidase enzyme reagent and peroxidase substrate (Santa Cruz Biotechnology, Inc., Santa Cruz, CA). Then, nuclei were stained with Mayer-hematoxilin (Wako, Osaka, Japan). Cells were examined for staining after rinsing with H_2O.

Radioiodide uptake assay

Cells were grown in six-well plates, washed with Hanks' balanced salt solution (HBSS), and incubated for 1 h at 37 C with 1000 μl HBSS containing 0.2 μCi carrier-free $Na^{125}I$ (Amersham Pharmacia Biotech, Piscataway, NJ) and 10 μM NaI with or without 300 μM $NaClO_4$ (34). The medium containing ^{125}I was removed, and the cell monolayer was washed twice with 1 ml HBSS. Cell-associated radioactivity of each sample was measured with a γ-counter after extraction with ethanol.

Radioiodide organification assay in vitro

After the BHP18–21v cells were incubated with 3 ng/ml depsipeptide, one of HDACI, for 72 h, 300 μM methimazole (MMI), a TPO-specific inhibitor, was added 24 h before the assay. Depsipeptide-treated BHP18–21v cells were then exposed to ^{125}I (0.2 μCi/well in six-well plates) in HBSS containing 10 μM NaI at 37 C for 1 h. Medium containing ^{125}I was removed and washed with fresh medium. Cell lysates were prepared with 1 ml of 0.1-N NaOH, and the radioiodide accumulation of the cells was measured with a γ-counter. Proteins in the cell lysates were precipitated by the addition of 1 ml TCA (final concentration, 20%). Assay tubes were centrifuged at 3300 × *g* for 30 min, and supernatants containing free radioiodide were removed. The precipitated proteins were washed again with 20% TCA, and radioactivity in the pellets were measured with a γ-counter. To measure the Tg- and TPO-independent nonspecific incorporation of ^{125}I into the protein fraction, iodination was measured in NIS-transfected FRTL-Tc, which expresses neither Tg nor TPO.

To investigate the molecular size of radioiodinated intracellular protein substrates, BHP18–21v cells, which were preincubated with or without 3 ng/ml depsipeptide for 48 h in a 10-cm culture dish, were exposed to ^{125}I (20 μCi/dish) in HBSS at 37 C for 1 h. Medium containing ^{125}I was removed and washed with fresh medium. Cell lysates were prepared with 1 ml of 0.1 N NaOH, and proteins in the cell lysates were precipitated by the addition of 1 ml TCA (final concentration, 20%), and pellets were washed again with 20% TCA. The cell pellets were dissolved with 100 μl of 10-mM HEPES/NaOH (pH 7.9), 0.1 mM EDTA, 1.5 mM $MgCl_2$, 10 mM KCl, 0.5 mM dithiothreitol, 1.5 mM phenylmethylsulfonylfluoride, and 10 μg/ml leupeptin. Thirty micrograms of protein extracts of lysate were resolved by SDS-PAGE (35) and processed for analysis by autoradiography. Radioactivity was analyzed using a BAS 2500 image analyzer (Fuji Film Co., Tokyo, Japan).

Analysis of iodide accumulation in vivo

A total of 1×10^7 BHP18–21v cells were transplanted in abdominal sc tissue of 8-wk-old male nude mice (BALB/C *nu/nu* mice). These mice were fed a low-iodide diet (Oriental Yeast, Tokyo, Japan) and were given 100 μg/kg·d L-T_4 (Wako) in their drinking water before the formation of tumors (8). Three weeks after the tumors reached approximately 1 cm in diameter, 5 μg/g·d depsipeptide or the vehicle, 0.1% DMSO (Sigma-Aldrich Corp., St. Louis, MO) in 100 μl PBS, was injected ip for 4 d. A total of 10 μCi $Na^{125}I$ (Amersham Pharmacia Biotech) in PBS was injected ip.

Three, 12, and 48 h later, the mice were killed, and radioactivity was analyzed with a BAS2500 image analyzer (Fuji Film Corp.). The mice were exposed to the imaging plates for 5 min. To investigate the ratio of tumor radioactivity to liver radioactivity, their tumors and organs were removed, and their weight and radioactivity were measured.

Three hours after injection of $Na^{125}I$, tumors were removed. Part of the tumor tissue was homogenated. After preparation of tissue lysate with 300 μl of 1-N NaOH, insoluble material was removed from the lysate by centrifugation at 3300 × *g* for 10 min at 4 C. Protein in the tissue lysates were precipitated by the addition of 600 μl of 40% TCA. The precipitated proteins were collected by centrifugation at 3300 × *g* for 20 min, and washed twice. Radioactivity in the pellets was measured with a γ-counter. Soluble protein was quantified by the Bradford method using RCDC Protein Assay (Bio-Rad Co., Hercules, CA).

Our institutional committee on animal care approved these studies.

Cytotoxic assay with depsipeptide treatment in vitro

Viabilities of cells treated with depsipeptide were measured with a nonradioactive cell proliferation assay, Cell Counting Kit-8 (Dojindo, Kumamoto, Japan). One day after plating 4×10^3 cells/well in triplicate wells of 96-well culture plates, cells were treated with 1, 3, and 10 ng/ml depsipeptide. Cell viability was assayed 48 h after incubation. Survival of cells is presented as a percentage of the absorbance with depsipeptide-treated cells divided by that with cells not exposed to depsipeptide.

Statistical analysis

All data are expressed as mean ± SEM. Differences between groups were examined for statistical significance using Student's *t* test and a *P* value < 0.05 was considered significant unless otherwise indicated.

Results

HDACI induced re-expression of NIS, TPO, and Tg mRNA in poorly differentiated and anaplastic thyroid cancer cells

To investigate the effects of the HDACI, the cancer cells were incubated with or without an HDACI for 24 h; then total RNA was isolated. Specifically, cells were incubated with 1, 3, and 10 ng/ml depsipeptide, strong HDACI (36), and expression of thyroid-specific genes was analyzed by quantitative real-time RT-PCR performed as described in *Materials and Methods* (Fig. 1A). In untreated BHP18–21v and ARO cells, we could observe neither expression of NIS, TPO, Tg, nor TSH-R. It should be additionally noted that faint expression of TPO and Tg mRNA in untreated ARO cells, and Tg mRNA in untreated BHP18–21v cells were detected, when the crossing points were set bellow 38 cycles. Addition of 3 and 10 ng/ml depsipeptide induced the expression of NIS, TPO, and Tg mRNA in BHP18–21v cells (Fig. 1A). In ARO cells, 3 and 10 ng/ml depsipeptide induced re-expression of NIS mRNA (Fig. 1A). TPO and Tg gene expression were induced by 1 ng/ml depsipeptide.

Additionally, BHP18–21v and ARO cells treated with at

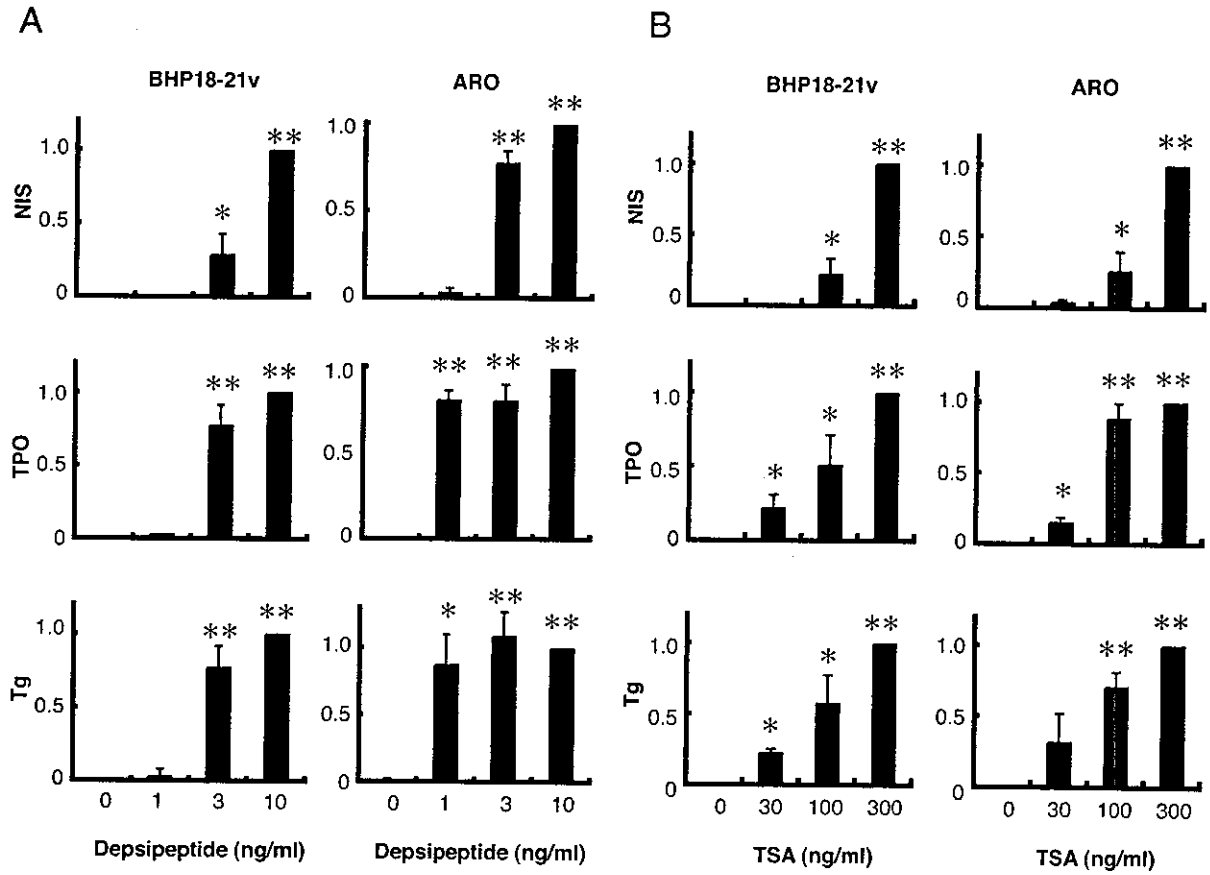

FIG. 1. The re-expression of NIS, TPO, and Tg mRNA induced by HDACI. A, Three thyroid-specific genes mRNA levels were assayed in BHP18–21v and ARO cells were incubated with 1, 3, or 10 ng/ml depsipeptide for 24 h. B, Three thyroid-specific genes mRNA levels were assayed in BHP18–21v, and ARO cells were incubated with 30, 100, or 300 ng/ml TSA for 72 h. From four independent samples, total RNA was isolated. Amounts of NIS, TPO, and Tg mRNA were determined by quantitative real-time RT-PCR with 100 ng cDNA in triplicate. Relative quantification of target cDNA was determined by arbitrarily setting the control value from maximum expression samples to 1. All data are expressed as the mean ± SEM. *, $P < 0.05$; **, $P < 0.001$, compared with untreated cells.

least 30 ng/ml trichostatin A (TSA) (Wako), which was also HDACI (37), expressed NIS, TPO, and Tg mRNA (Fig. 1B). These results indicate that HDACI induced the restoration of thyroid-specific gene expression that had been lost in the process of oncogenesis.

We also investigated time dependence of the HDACI-induced expression of thyroid-specific genes. Amounts of thyroid-specific genes mRNA reached a maximum 48 h after addition of 3 ng/ml depsipeptide to BHP18–21v cells. In ARO cells, re-expression of NIS and TPO reached a maximum after 12 h, whereas Tg gene gradually increased and peaked 48 h after the incubation with 3 ng/ml of depsipeptide (Fig. 2).

HDACI induces radioiodide uptake in BHP18–21v and ARO cells

Radioiodide uptake was measured in an effort to determine whether depsipeptide-induced NIS mRNA yielded a functional protein. After 48 h treatment with depsipeptide, BHP18–21v and ARO cells were incubated with $Na^{125}I$ (0.2 μCi/well) with or without 300 μM sodium perchlorate for 1 h (Fig. 3, A and B). In nontreated BHP18–21v and ARO cells, no difference in intracellular radioactivity was seen in cells with or without addition of sodium perchlorate, specific inhibitor. This result indicated that the cell line had lost its ability to take up iodide via NIS protein in thyroid cancer cells.

BHP18–21v cells incubated with 1 ng/ml depsipeptide showed a small increase in radioiodide uptake. However, there were no significant differences compared with sodium perchlorate-treated cells. Treatment with 3 and 10 ng/ml depsipeptide induced significant radioiodide uptake in BHP18–21v cells (Fig. 3A). This radioiodide uptake was inhibited by sodium perchlorate. In ARO cells, incubation with 1 ng/ml depsipeptide induced no radioiodide accumulation; 3 and 10 ng/ml of depsipeptide increased the count of radioiodide uptake (Fig. 3B). These results showed that the depsipeptide induced significant iodide uptake that was mediated by newly produced NIS protein. These results agreed with the findings in quantitative real-time RT-PCR (Fig. 1) that induction of NIS mRNA was required for at least 3 ng/ml depsipeptide.

To evaluate the effect of TSH, we performed the iodide uptake assay pretreated with or without TSH. There were no

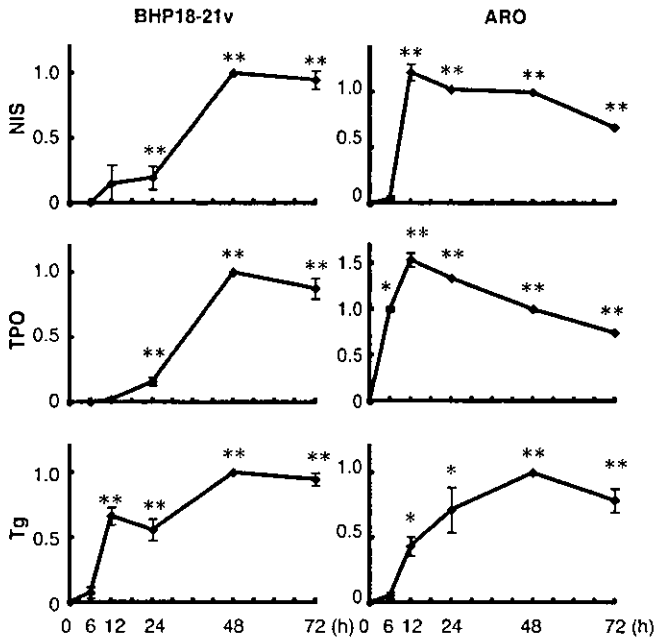

FIG. 2. Time-dependent expression of thyroid-specific genes mRNA. Re-expression of thyroid-specific genes was analyzed in BHP18–21v and ARO cells incubated with 3 ng/ml depsipeptide for 12, 24, 48, or 72 h. Total RNA was isolated in three independent samples. Amounts of thyroid-specific genes mRNA were determined by quantitative real-time RT-PCR with 100 ng cDNA in triplicate. Relative quantification of target cDNA was determined by arbitrarily setting the control value of samples at 48 h incubation to 1. All data are expressed as the mean ± SEM. *, $P < 0.05$, compared with control cells; **, $P < 0.001$, compared with controls cells.

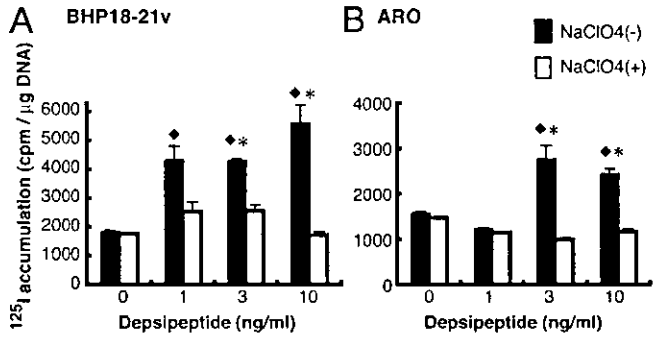

FIG. 3. Characterization of radioiodide uptake in BHP18–21v and ARO cells incubated with depsipeptide. A, BHP18–21v cells were incubated with depsipeptide for 48 h. B, ARO cells were incubated with depsipeptide for 48 h. These cancer cells were incubated in 0.2 μCi $Na^{125}I$-containing medium with or without 300 μM of $NaClO_4$ for 1 h. Cells were washed twice with ice-cold HBSS and exposed to 100% ethanol. Extracted radioactivity was measured with a γ-counter. All data are expressed as the mean ± SEM (n = 9). ♦, $P < 0.01$, compared with untreated cells; *, $P < 0.01$, compared with $NaClO_4$-treated cells.

differences in the amount of depsipeptide-induced iodide uptake between TSH-treated and untreated cells (data not shown). In addition, no expression of TSH-R mRNA was observed in either depsipeptide- or TSA-treated BHP18–21v or ARO cells (data not shown). These results indicate that TSH-R gene expression is hardly influenced by HDACI, and depsipeptide-induced iodide uptake is TSH-independent.

Immunocytochemical demonstration of HDACI-induced NIS, TPO, and Tg proteins expression in BHP18–21v and ARO cells

To analyze whether HDACI-up-regulated NIS, TPO, or Tg mRNAs is translated to corresponding protein product, immunoreactive NIS, TPO, or Tg proteins expressed in BHP18–21v and ARO cells were stained with anti-NIS, anti-TPO, or anti-Tg antibody. The presence of the NIS protein was detected by immunocytochemistry in HDACI-treated BHP18–21v and ARO cells and was observed in the cell membrane and cytosol (Fig. 4, B, C, K, and L). On the contrary, untreated cells were not stained (Fig. 4, A and J). Treatment with anti-TPO antibody did not yield any staining in BHP18–21v or ARO cells untreated with HDACI (Fig. 4, D and M). In contrast, marked staining was observed in both cell lines treated with HDACI (depsipeptide at 3 ng/ml or TSA at 300 ng/ml) for 48 h (Fig. 4, E, F, N, and O). This TPO immunostaining was localized in the region of cell membrane and cytosol. Expressed immunoreactive Tg protein also was stained with anti-Tg monoclonal antibody in BHP18–21v and ARO cells treated with depsipeptide (3 ng/ml) or TSA (300 ng/ml). Tg protein was detected in the area of the cytosol (Fig. 4, H, I, Q, and R). No Tg staining was observed in untreated cells (Fig. 4, G and P). These results clearly show that HDACI induced the expression of NIS, TPO, and Tg proteins, whereas re-expressed NIS and TPO protein were localized in either region of cell membrane and cytosol.

HDACI augments radioiodide organification in BHP18–21v cells

As described above, we demonstrated that HDACI induced the re-expression of NIS, TPO, and Tg protein. To confirm the function of the expressed TPO and Tg, we measured HDACI-induced radioiodide organification. BHP18–21v cells were incubated with 1, 3, and 10 ng/ml depsipeptide for 48 h. MMI (300 μM), which inhibits the TPO-induced

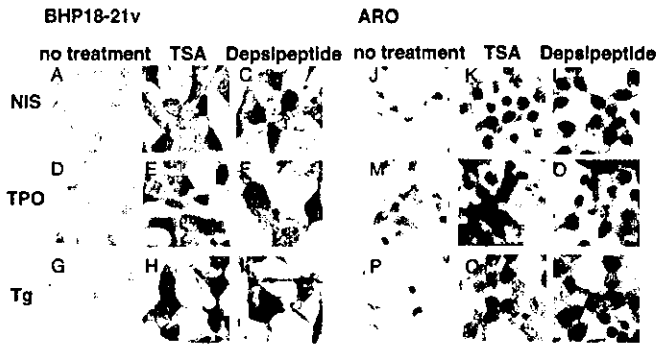

FIG. 4. Detection of immunoreactive NIS, TPO, and Tg proteins in HDACI-treated BHP18–21v and ARO thyroid cancer cells. BHP18–21v and ARO cells were incubated for 48 h with 3 ng/ml depsipeptide or 300 ng/ml TSA. A–C and J–L, The presence of NIS protein was examined by immunostaining using an anti-NIS monoclonal antibody in BHP18–21v and ARO cells treated with or without HDACI. D–F and M–O, The fixed cells were stained with an anti-TPO monoclonal antibody. G–I and P–R, Tg immunostaining was examined in cells incubated with or without HDACI. The fixed cells were incubated with an anti-NIS, anti-TPO, and anti-Tg monoclonal antibody and then a biotinylated secondary antibody, and then stained with avidin-biotinylated horseradish peroxidase.